

# Tradeoff Between Ergodic Energy Efficiency and Spectral Efficiency in D2D Communications Under Rician Fading Channel

Mohammad Robat Mili <sup>1</sup>, Ata Khalili <sup>2</sup>, *Graduate Student Member, IEEE*, Nader Mokari, *Senior Member, IEEE*, Sabine Wittevrongel <sup>3</sup>, Derrick Wing Kwan Ng <sup>4</sup>, *Senior Member, IEEE*, and Heidi Steendam <sup>5</sup>, *Senior Member, IEEE*

**Abstract**—This paper aims at investigating the tradeoff between ergodic energy efficiency (EE) and spectral efficiency (SE) for device-to-device (D2D) communications underlying cellular networks. Assuming average-based resource allocation, we propose a multiobjective optimization problem (MOOP) approach to deal with the EE and SE maximization problem. Specifically, the formulated MOOP results in the maximization of the total ergodic sum rate of the D2D users and the minimization of the total average transmit power of the D2D transmitters. Two practical scenarios are considered, i.e., a limited interference scenario, which includes the sparsely deployed scenario, and a densely deployed scenario, where for each scenario the maximum achievable EE and SE are derived. Specifically, considering the limited interference scenario, an upper bound is imposed on the received interference across different D2D communications, and closed-form expressions for the optimal power allocation, ergodic sum rate, and maximum EE are obtained. In the general, densely deployed scenario, however, the cross D2D network interference needs to be taken into account. We provide an optimal solution for the power control based on sequential fractional programming to tradeoff between complexity and performance gain. Simulation results unveil an interesting tradeoff to strike a balance between EE and SE.

**Index Terms**—Device-to-device (D2D) communications, energy efficiency, spectral efficiency, multiobjective optimization, tradeoff.

Manuscript received September 30, 2019; revised February 15, 2020 and May 1, 2020; accepted June 9, 2020. Date of publication June 12, 2020; date of current version October 13, 2020. This work was supported in part by the EOS under Grant 30452698 from the Belgian Research Councils FWO and FNRS and in part by the Flemish Government (AI Research Program). The work of Derrick Wing Kwan Ng was supported in part by the UNSW Digital Grid Futures Institute, UNSW, Sydney, under a cross-disciplinary fund scheme, and in part by the Australian Research Council's Discovery Project (DP190101363). The review of this article was coordinated by Dr. J. Liu. (*Corresponding author: Mohammad Robat Mili.*)

Mohammad Robat Mili and Sabine Wittevrongel are with the Department of Telecommunications and Information Processing, Ghent University, 9000 Gent, Belgium (e-mail: Mohammad.Robatmili@ieee.org; Sabine.Wittevrongel@ugent.be).

Ata Khalili is with the Department of Electrical and Computer Engineering, Tarbiat Modares University, Tehran 14115-111, Iran, and also with the Electronics Research Institute, Sharif University of Technology, Tehran 19166, Iran (e-mail: ata.khalili@ieee.org).

Nader Mokari is with the Department of Electrical and Computer Engineering, Tarbiat Modares University, Tehran 14115-111, Iran (e-mail: nader.mokari@modares.ac.ir).

Derrick Wing Kwan Ng is with the School of Electrical Engineering and Telecommunications, University of New South Wales, Sydney, NSW 2052, Australia (e-mail: w.k.ng@unsw.edu.au).

Heidi Steendam is with the Department of Telecommunications and Information Processing (TELIN-IPI/IMEC), Ghent University, 9000 Gent, Belgium (e-mail: Heidi.Steendam@ugent.be).

Digital Object Identifier 10.1109/TVT.2020.3002296

## I. INTRODUCTION

IN RECENT years, the rapid growth of smart devices and new applications leads to an increasing demand for high data transmission rate in mobile wireless networks. The traditional architecture of cellular systems will not be able to sufficiently support the upcoming increase in mobile data traffic [1]. Device-to-device (D2D) communications have emerged as a promising technology to increase the overall spectral efficiency of cellular networks and improve the connectivity of devices without extra construction and maintenance costs. This technology offers the possibility to setup a direct link between two users within the cellular coverage without the help of the base station, enabling to offload the data traffic between the base station and users [2], [3]. Also, D2D communication with a software defined network can enhance user quality of experience by improving the success probability of internet access [4]. D2D communication works either in overlay or underlay mode with cellular users. In the overlay mode, a dedicated spectrum is utilized for D2D users, whereas in the underlay mode, the spectrum is shared between the D2D users and cellular users [5]. In the underlay mode, higher spectral efficiency and total rate can be obtained. However, mutual interference, due to reusing the resources between D2D links and cellular users, occurs and needs to be managed, as it affects the performance of both types of users. Furthermore, D2D communication can be considered as a crucial enabler of the Internet of Things (IoT), where devices are able to communicate with each other directly. In D2D based IoT network, ultra-reliable low latency communication is a vital aspect of wireless connectivity. As a result, the application of D2D for IoT was discussed in [6]–[10].

Future generation wireless networks not only struggle with limited spectrum resources, but also face the challenge to operate with limited batteries. Recently, energy-efficient communication systems, or the well-known Green Radios, have been attracting growing attention from the research community due to their ability to improve the system performance while simultaneously reducing the energy consumption of the communication devices. Limiting the energy consumption of wireless networks is important not only to prolong battery lives, but also because of environmental concerns. Information and communication technology (ICT) is responsible for more than

2% of the whole world CO<sub>2</sub> gas emission [11]. To minimize the carbon footprint of ICT, thus its environmental impact [14], we need new and efficient communication techniques. In the recent literature, energy efficiency (EE), that measures the number of bits communicated per unit of energy consumed, has emerged as the performance metric to evaluate the communication system energy consumption [12]–[17]. For instance the problem of bandwidth allocation, relay selection, and power allocation was investigated in [18] to enhance the weighted sum energy efficiency while guaranteeing the minimum data rate for cellular users. By exploiting the theory of fractional programming, the considered problem was transformed into a more tractable equivalent problem where a solution based on the Lagrange dual method was developed. In [19], the performance tradeoff in relay aided D2D-cellular networks was investigated, where the optimal transmit powers of both source and relay users were derived. The work in [20] studied the tradeoff between EE and spectral efficiency (SE) for underlaying mobile D2D communications, where two power allocation schemes were proposed to characterize the impact of vehicular environments on both EE and SE. The geometric water-filling approach was adopted in [21] to optimize the transmission rate of the D2D users in terms of throughput maximization, while an adaptive subcarrier allocation was proposed. In [22], subchannel allocation and power optimization were considered, where the queuing delay was flexibly managed to optimize the EE-SE maximization in D2D communications underlaying cellular networks. Furthermore, power allocation for D2D communication was investigated to mitigate cross-tier interference arising from co-channels based on the stochastic geometry [23]–[25]. In this regard, the works [23], [24] took into account minimum received power, relative deployment density, transmit power control, and channel allocation. In these works, a stochastic geometry based theoretical framework to analyze the coverage probability and ergodic rate for respectively the uplink and downlink of a D2D overlaying multi-channel was considered. In [23], a framework based on the stochastic geometry for D2D multi-cell overlaying uplink cellular network is presented to characterize the coverage probability and ergodic rate of D2D overlaying multi-channel uplink cellular networks with minimum received power and channel allocation. On the other hand, [24] proposed a new scheme for a D2D overlaying multi-channel downlink in which two users communicate with each other in either one-hop or two-hop mode. In [25], the authors derived the spatial average rate, success probability, and area spectral efficiency performances for both cellular users and D2D users under Rician fading, specifically employing stochastic geometry as an analysis framework. In [26], the joint power and channel allocation problem for D2D over Rician fading D2D channels was investigated while maximizing the sum rate of cellular users subject to the rate constraints for cellular users as well as the outage probability and latency constraints for D2D users.

Current system design problems are mostly dealing with conflicting requirements, e.g., the need to increase the system throughput, while at the same time limiting the energy

consumption and the end-to-end delay. A multi-objective optimization problem (MOOP) formulation, which focuses on the simultaneous optimization of two or more conflicting objective functions for which the most preferred solution needs to be chosen in the presence of tradeoffs between them [27], is one way to deal with such problems. Recently, several MOOP solutions have been proposed to observe the correlation between different objectives in wireless communications [28]–[37]. In this regard, a multi-objective cell association optimization for arranging a number of D2D links in a multi-cell network based on the fractional frequency reuse scheme was considered in [29]. In [33], interference efficiency as a new performance metric in underlay cognitive radio networks was introduced and then optimized by formulating a MOOP. In [35], a MOOP formulation was used to maximize the EE of a single-cell wireless network. Since EE is a key parameter in designing future wireless networks, energy-aware system design as an immediate challenge is necessary in industry and academia. Bandwidth expansion improves the EE but decreases the spectral efficiency, so it is vital to achieve a balance between EE and SE as conflicting objectives. Recently, the tradeoff between EE and SE of wireless communications as a MOOP is investigated in [37]–[38]. The authors in [37] formulated a MOOP to maximize simultaneously the global EE and SE while guaranteeing individual operator constraints, e.g. quality of service and energy consumption in a network where radio resources were shared among multiple operators. A MOOP tradeoff in D2D communications underlaying heterogeneous networks was studied in [38] to strike a balance between EE and SE. This problem was transformed into a single objective optimization problem (SOOP) via an epsilon method and a two-stage iterative solution was proposed. Optimizing the resource allocation of D2D communications for multicell environments with intercell interference, while taking into account multi-cell interference and long term channel information, has been proved challenging in the literature e.g. [14]–[17], [35]–[38]. To our best knowledge, the tradeoff between ergodic EE and SE in D2D communications has never been discussed. Therefore, in this paper, we focus on jointly maximizing the EE and ergodic sum rate in underlay D2D communications. To this end, we formulate a MOOP that jointly maximizes the ergodic sum rate of the D2D links and minimizes the total average power of the D2D transmitters under an average received power constraint (at the cellular receivers) and per-D2D-user transmit power constraints. In detail, we provide a framework for the optimal power allocation in D2D communications underlaying a multicellular network, where cellular users (CUs) communicate with the base stations using an orthogonal frequency division multiple access (OFDMA) technique. The D2D users, operating within the coverage area of the base stations, share the radio spectrum with the CUs and communicate with each other.

In summary, the main goal of this paper is to optimize the ergodic EE and SE in multicell D2D communications. The main contributions of our paper are summarized as follows:

- We aim to investigate the tradeoff between the ergodic EE and SE maximization in D2D communications underlaying

with a cellular downlink network, taking into account the constraints on the average interference power received at the CUs and transmit power of each D2D user. To this end, we transform the EE-SE maximization objectives into a MOOP that jointly maximizes the ergodic sum rate of the D2D links and minimizes the total average power of D2D transmitters, and solve the obtained MOOP via the weighted Tchebycheff method.

- Starting from this MOOP, we further develop the power allocation for two types of practical D2D network models, namely, a limited interference case, including the sparsely deployed scenario, and the general case corresponding to a densely deployed scenario. For the first case, an upper bound is imposed on the interference across different D2D communications, and in the case of a sparsely deployed scenario, this cross-interference even is neglected. A new closed-form expression for the power allocation is obtained. In the densely deployed scenario, cross interference is not upper limited and may significantly affect the system performance. For this case, we propose an iterative technique to solve the non-convex MOOP suboptimally. Furthermore, the computational complexity of the proposed solution method is investigated.
- We provide an optimal power allocation via sequential fraction programming and compare the results obtained via the MOOP and sequential fractional programming to strike a balance between computational complexity and optimality.
- With the aid of numerical simulations, we analyze the tradeoff between EE and SE D2D communications underlying cellular downlink networks. Besides, we study the system performance in both Rician fading channels and Rayleigh fading channels and analyze the differences.

The paper is organized as follows. Section II describes the system model. Section III formulates the MOOP. Section IV proposes the closed-form expressions for the limited interference scenario, while Section V considers a solution for the densely deployed scenario. Section VI discusses a power allocation solution based on sequential fractional programming. The computational complexity of the given methods is studied in Section VII. Numerical results are presented in Section VIII, followed by some concluding remarks in Section IX.

## II. SYSTEM MODEL

We consider D2D communications underlying a multicellular downlink network with  $C$  cells denoted by  $\mathcal{C} = \{1, 2, \dots, C\}$ , i.e., multiple D2D pairs and CUs share the same frequency bands in each cell. Each cell has one base station and multiple CUs, and each subchannel is used by one CU within each cell only. D2D users in each cell communicate with each other through a point-to-point link and compete for the set of available subchannels. We assume that in this cellular network, there are  $K$  CUs that operate in the presence of  $M = \sum_{c=1}^C M_c$  D2D links, where  $M_c$  is the number of D2D links in cell  $c$ . The total available bandwidth  $B_T$  Hz is divided into  $N$  non-overlapping subchannels, each comprising a bandwidth  $B = B_T/N$  Hz, and

indexed by  $n \in \mathcal{N} = \{1, 2, \dots, N\}$ . In order to avoid harmful interference to the CUs, D2D transmitters must control their transmit power so that the interference constraint imposed by the CUs is satisfied. The D2D transmitter  $i$  sends a signal with power  $P_i^{(n)}$  over subchannel  $n$ . The macro-BS has perfect channel state information (CSI) of all links and can schedule proper power allocation. In fact, the CSI of all users is assumed to be perfectly known at the macro-BS so as to unveil the performance upper bound of the system. In this system, the instantaneous received signal-to-interference-plus-noise ratio (SINR) at the D2D receiver  $i$  on subchannel  $n$  can be obtained using the following formula:<sup>1</sup>

$$\text{SINR}_i^{(n)} = \frac{P_i^{(n)} h_{ii}^{(n)}}{N_0 B + \sum_{c=1}^C \rho_c^{(n)} g_{ci}^{(n)} + \sum_{\substack{j=1 \\ j \neq i}}^M P_j^{(n)} h_{ji}^{(n)}}, \quad (1)$$

where  $h_{ii}^{(n)}$  represents the instantaneous channel power gain of the link between the  $i$ th D2D transmitter and receiver, which is assumed to be flat fading with additive white Gaussian noise (AWGN) with distribution  $CN(0, N_0)$  (zero-mean circularly symmetric complex Gaussian noise with variance  $N_0$ ). The transmit power of the base station  $c$  on subchannel  $n$  is denoted by  $\rho_c^{(n)}$ .  $g_{ci}^{(n)}$  is an intercell interference channel power gain between the base station and the D2D receiver  $i$ . The channel power gain  $h_{ji}^{(n)}$  denotes an intercell interference channel power gain between another D2D transmitter  $j$  and the D2D receiver  $i$ , all on the same subchannel  $n$ . The interference terms  $P_{CU,i}^{(n)} = \sum_{c=1}^C \rho_c^{(n)} g_{ci}^{(n)}$  and  $P_{DU,i}^{(n)} = \sum_{\substack{j=1 \\ j \neq i}}^M P_j^{(n)} h_{ji}^{(n)}$  collect all interference contributions from the base stations and other D2D links, respectively. To simplify the notation, we define  $NI_i^{(n)} = N_0 B + P_{CU,i}^{(n)} + P_{DU,i}^{(n)}$  and  $NI_{CU,i}^{(n)} = N_0 B + P_{CU,i}^{(n)}$ . The key notations are summarized in Table I.

Note that the above model for direct D2D links also can be used to characterize vehicle-to-vehicle (V2V) communication links. Similarly, as D2D, V2V communication is intended for short-range communication. Important aspects in V2V are low latency and high reliability. As in the above model, information is exchanged using a single hop, this latency can be kept small. Further, due to the short range, the D2D link enables high bit rates and low power consumption.

## III. JOINTLY MAXIMIZING EE AND SE

In this section, following a similar approach as used in [19]–[22] to manage interference between CUs and D2D links, we jointly maximize the EE and SE<sup>2</sup> of the D2D communications in a fading environment, while satisfying a target on each D2D user average transmit power and received power constraints at the CUs. We define the ergodic sum rate for transmitter  $i$  as

$$R_{DU,i} = \sum_{n=1}^N \chi_i^{(n)} \mathbb{E}[\ln(1 + \text{SINR}_i^{(n)})]. \quad (2)$$

<sup>1</sup>We note that in the expressions, the time index has been omitted for ease of notation.

<sup>2</sup>In this paper we define the system SE (bit/s/Hz) as the sum rate of all D2D users.

TABLE I  
TABLE OF NOTATIONS

Notation	Description
$\mathcal{C}$	Set of cellular BS
$K$	Number of cellular users
$M$	Number of D2D links
$\mathcal{N}$	Set of subchannels
$P_{\max}(i)$	Maximum allowable transmit power of each D2D user
$P_i^{(n)}$	Transmit power of D2D user $i$ over subchannel $n$
$\chi_i^{(n)}$	Subchannel assignment variable
$\rho_c^{(n)}$	Transmit power of BS $c$ over subchannel $n$
$h_{ii}^n$	Channel power gain of the link between the $i$ -th D2D transmitter and receiver.
$h_{ji}^n$	Intercell interference channel power gain from another D2D transmitter $j$ to D2D receiver $i$
$f_{ik^*}^{(n)}$	Channel power gain of the link between the $i$ th D2D transmitter and the $k^*$ th CU over subchannel $n$
$R_{\min}$	Minimum data rate requirement for D2D users
$Q_{k^* \max}$	Average interference power caused by the D2D users towards CU $k$ on each subchannel
$P_{DU, I_{\text{th}}}$	Maximum interference arising from D2D links
$P_C$	Total circuit power consumption

Then, the EE and SE maximization problem is formulated as

$$\max_{\mathbf{P}, \chi} \text{EE} = \frac{\text{SE}}{P_{\text{Total}}}, \quad (3a)$$

$$\max_{\mathbf{P}, \chi} \text{SE} = \sum_{i=1}^M R_{\text{DU}, i}, \quad (3b)$$

$$\text{s.t.: } \bar{\mathbf{P}}(i) = \sum_{n=1}^N \chi_i^{(n)} \mathbb{E}[P_i^{(n)}] \leq P_{\max}(i), \quad (3c)$$

$$\forall i \in \{1, 2, \dots, M\},$$

$$\mathbf{Q} = \sum_{i=1}^M \chi_i^{(n)} \mathbb{E}[P_i^{(n)} f_{ik^*}^{(n)}] \leq Q_{k^* \max}, \quad \forall n \in \mathcal{N}, \quad (3d)$$

$$R_{\text{DU}, i} \geq R_{\min}, \quad \forall i \in \{1, 2, \dots, M\} \quad (3e)$$

$$\sum_{i=1}^{M_c} \chi_i^{(n)} \leq 1, \quad \forall n \in \mathcal{N}, \forall c \in \mathcal{C}, \quad (3f)$$

$$\chi_i^{(n)} \in \{0, 1\}, \quad \forall n \in \mathcal{N}, \forall i \in \{1, 2, \dots, M\}, \quad (3g)$$

where

$$P_{\text{Total}} = \sum_{i=1}^M \sum_{n=1}^N \epsilon_i \chi_i^{(n)} \mathbb{E}[P_i^{(n)}] + P_C \quad (4)$$

is the total transmission power of the D2D transmitters, in which  $\epsilon_i$  is the power amplifier efficiency of the  $i$ -th D2D user. Further,  $P_C$  is the total circuit power consumption which is calculated as  $P_C = \sum_{i=1}^M P_{C_i}$ , in which  $P_{C_i}$  is a constant value denoting the circuit power consumption of D2D user  $i$ . The

parameters to be determined in this optimization problem are the matrix  $\mathbf{P} \in \mathbb{R}^{M \times N}$ , containing the power allocation variables  $P_i^{(n)}, i = 1, \dots, M, n = 1, \dots, N$ , and the matrix  $\chi \in \mathbb{Z}^{M \times N}$ , containing the subchannel assignment variables for the D2D users. In (3),  $\mathbb{E}[\cdot]$  denotes the averaging operator. To find the optimum  $\mathbf{P}$  and  $\chi$ , the EE (3a) and ergodic sum rate SE (3b) are maximized subject to the condition that the average power  $\bar{\mathbf{P}}(i)$  of the  $i$ th D2D user is upper limited by  $P_{\max}(i)$  (3c), the total average interference power caused by the D2D users towards CU  $k$  on each subchannel must be smaller than  $Q_{k^* \max}$  with  $k^* = \arg \min_k Q_{k \max}$  (3d),<sup>3</sup> and the ergodic sum rate  $R_{\text{DU}, i}$  of each D2D user must exceed the minimum rate  $R_{\min}$  (3e). The last two conditions are related to the subchannel assignment variables  $\chi_i^{(n)}$ , which are binary variables where  $\chi_i^{(n)} = 1$  if subchannel  $n$  is allocated to D2D user  $i$ , and  $\chi_i^{(n)} = 0$  otherwise. Condition (3f) indicates that in each cell, each subchannel  $n$  is allocated to at most a single D2D user. In (3d),  $f_{ik^*}^{(n)}$  denotes the channel power gain of the link between the  $i$ th D2D transmitter and the  $k^*$ th CU over subchannel  $n$ .

To find the optimal power allocation in a subchannel, the EE and ergodic sum rate maximization problem will be solved in two steps. In the first step, we convert the EE maximization objective, given in (3a), into two objectives. In the second step, the formulated MOOP is solved by converting it into an equivalent SOOP by using the weighted Tchebycheff method. In the following, we explain these steps in detail.

First, we reformulate the objective function (3a) into the following objectives that jointly maximize the total ergodic sum rate SE of the D2D communications (which also equals the objective (3b)) and minimize the total transmission power  $P_{\text{Total}}$  as

$$\max_{\mathbf{P}, \chi} \text{SE} \quad (5a)$$

$$\min_{\mathbf{P}, \chi} P_{\text{Total}}. \quad (5b)$$

A well known technique to solve a MOOP is the weighted Tchebycheff method [27]–[32], which introduces an additional auxiliary optimization variable  $\psi$  given as follows:

$$\min_{\mathbf{P}, \chi, \psi} \psi \quad (6a)$$

$$\text{s.t.: } \frac{\eta}{C_0} (C_0 - \text{SE}) - \psi \leq 0, \quad (6b)$$

$$\left( \frac{1 - \eta}{P_0} \right) (P_{\text{Total}} - P_0) - \psi \leq 0, \quad (6c)$$

$$(3c) - (3g),$$

where  $C_0$  and  $P_0$  are the optimal objective values with respect to each objective i.e., the maximum of the total ergodic sum rate of the D2D communications and the minimum of the total transmission power of D2D transmitters, respectively. Moreover,  $\eta$

<sup>3</sup>The inequality constraint (3d) on the interference power imposes  $\bar{\mathbf{Q}} = \sum_{i=1}^M \chi_i^{(n)} \mathbb{E}[P_i^{(n)} f_{ik^*}^{(n)}] \leq Q_{k \max}$ , where  $Q_{k \max}$  is the maximum tolerable interference power from the D2D users to the  $k$ -th CU  $\forall k$ . However, due to the high computational complexity involved with this constraint, we tighten the constraint by imposing  $Q \leq Q_{k^* \max}$  where  $k^* = \arg \min_k Q_{k \max}$  [39].

and  $(1 - \eta)$  denote the weighting coefficients indicating the importance of the different objectives. The closer  $\eta$  gets to one, the more weight the ergodic sum rate gets in the optimization, and for small  $\eta$ , the total transmission power is more important. By changing  $\eta$  from 0 to 1, all points on the Pareto bound are obtained. It is worth mentioning that the weighted Tchebycheff method guarantees to generate a set of Pareto-optimal solutions by varying the weights, even if the MOOP is non-convex [27], [28].

Note that even though the power is minimized in (5) as part of the MOOP objectives, constraining the power (3c) is still required. Although the optimal operational power level will change depending on the level of priority allocated to the different objectives in the MOOP, this optimum not necessarily is a small value. As a result, the MOOP optimum operational power may settle for a level that is beyond the battery limit of the transmitters. By constraining the maximum power in (3c), we prevent this to happen.

The ergodic sum rate (2) will be affected by the presence of interference from both the CU and other D2D links. Depending on the level of the interference, different solution methods must be considered. In the next two sections, we consider two scenarios, i.e. the scenario with limited interference and the densely deployed scenario.

#### IV. OPTIMIZATION PROBLEM FOR THE CASE WITH LIMITED INTERFERENCE

In this scenario, we assume that the interference between D2D users is limited, i.e.,

$$P_{DU,i}^{(n)} = \sum_{\substack{j=1 \\ j \neq i}}^M P_j^{(n)} h_{ji}^{(n)} \leq P_{DU,I_{Th}}, \forall i, \quad (6e)$$

where  $P_{DU,I_{Th}}$  is the maximum interference arising from D2D links, which is also known as interference temperature. This scenario can be used in several practical scenarios, e.g. in a sparsely deployed scenario, where the interference can safely be ignored, implying  $P_{DU,i}^{(n)} = 0^4$ , and in a dense urban high rise scenario. Although in this latter scenario the density of subscribers is high, the interference between D2D users is limited due to the presence of tall buildings, causing a strong attenuation of D2D signals that are not nearby. The amount of interference can be controlled in each subchannel  $n$ , by varying the value of  $P_{DU,I_{Th}}$ . This flexibility leads to an improvement of the system performance.

In this scenario, we impose constraint (6e) to the optimization problem (6). Hence, the lower bound on the received SINR in subchannel  $n$  at D2D receiver  $i$  can be expressed using the following equation:

$$\text{SINR}_{i,\text{Lower}}^{(n)} = \frac{P_i^{(n)} h_{ii}^{(n)}}{NI_{CU,i}^{(n)} + P_{DU,I_{Th}}}. \quad (7)$$

<sup>4</sup>This implies the channel gains between D2D links are assumed to be zero, due to the large distance between D2D users in the sparse scenario.

By replacing the SINR value in (1) with  $\text{SINR}_{i,\text{Lower}}^{(n)}$  given in (7), the data rate function becomes concave with respect to the optimization variables. However, the optimization problem (6) is still non-convex, due to the binary subchannel allocation variables  $\chi$ . Hence it is computationally prohibitive to give an optimal solution. To solve this issue, we relax the binary constraint of the subchannel assignment indicator in (3g) into a continuous one in the interval  $[0,1]$ , which allows us to derive a computationally efficient power and subchannel allocation. Hence, in the new definition,  $\chi_i^{(n)}$  can represent the fraction of time that subchannel  $n$  is allocated to the  $i$ th D2D link. As a result of the time sharing condition discussed in [40] and [41], strong duality holds in multicarrier systems despite of the non-convexity of the optimization problem. Moreover, although we apply binary constraint relaxation to the subchannel allocation variables, the optimal subchannel allocation for the constraint relaxed problem is still binary, i.e., the constraint relaxation is tight. We further introduce a new variable  $\hat{P}_i^{(n)} = P_i^{(n)} \chi_i^{(n)}$  representing the actual amount of allocated power to the D2D transmitter  $i$  on subchannel  $n$ . Consequently, (6) is transformed into

$$\min_{\hat{\mathbf{P}}, \chi, \psi} \psi \quad (8a)$$

$$\text{s.t.: } \eta \left( C_0 - \sum_{i=1}^M \sum_{n=1}^N \chi_i^{(n)} \mathbb{E} \left[ \ln \left( 1 + \frac{\hat{P}_i^{(n)} h_{ii}^{(n)}}{\chi_i^{(n)} \left( NI_{CU,i}^{(n)} + P_{DU,I_{Th}} \right)} \right) \right] \right) - \psi \leq 0, \quad (8b)$$

$$(1 - \eta) \left( \sum_{i=1}^M \sum_{n=1}^N \epsilon_i \mathbb{E}[\hat{P}_i^{(n)}] + P_C - P_0 \right) - \psi \leq 0, \quad (8c)$$

$$\sum_{n=1}^N \mathbb{E}[\hat{P}_i^{(n)}] \leq P_{\max}(i), \forall i \in \{1, 2, \dots, M\}, \quad (8d)$$

$$\sum_{i=1}^M \mathbb{E}[\hat{P}_i^{(n)} f_{ik^*}^{(n)}] \leq Q_{k^* \max}, \forall n \in \mathcal{N}, \quad (8e)$$

$$\sum_{n=1}^N \chi_i^{(n)} \mathbb{E} \left[ \ln \left( 1 + \frac{\hat{P}_i^{(n)} h_{ii}^{(n)}}{\chi_i^{(n)} \left( NI_{CU,i}^{(n)} + P_{DU,I_{Th}} \right)} \right) \right] \geq R_{\min}, \quad (8f)$$

$$(3f), (3g), (6e)$$

where  $\hat{\mathbf{P}} \in \mathbb{R}^{M \times N}$  is the matrix containing the power allocation variables  $\hat{P}_i^{(n)}$ ,  $i = 1, \dots, M$ ,  $n = 1, \dots, N$ . Now, (8) is a convex optimization problem, for which a unique optimal solution can be obtained using the Lagrange dual function. Forming the Lagrangian, taking the derivative of the Lagrangian with respect to  $\hat{P}_i^{(n)}$  and setting the derivative equal to zero, the transmit power  $\hat{P}_i^{(n)}$  is obtained [42]. After some straightforward computations, we find

$$P_i^{(n)} = \frac{\hat{P}_i^{(n)}}{\chi_i^{(n)}} = \left[ \frac{\eta\lambda + \omega_i}{(\nu_i + v - \eta v) + f_{ik^*}^{(n)}\mu_n + \phi_{i,n}h_{ji}^{(n)}} - \frac{NI_{CU,i}^{(n)} + P_{DU,I_{Th}}}{h_{ii}^{(n)}} \right]^+, \quad (9)$$

where  $\lambda, v, \boldsymbol{\nu} = (\nu_1, \nu_2, \dots, \nu_M), \boldsymbol{\mu}, \boldsymbol{\omega}$ , and  $\phi$  are non-negative Lagrangian dual variables corresponding to the constraints (8b), (8c), (8d), (8e), (8f), and (6e), respectively, and  $[\cdot]^+$  stands for  $\max\{0, \cdot\}$ . Note that the power allocation  $P_i^{(n)}$ , i.e., the instantaneous power at the  $i$ th D2D transmitter in subchannel  $n$ , is a function of  $h_{ii}^{(n)}, f_{ik^*}^{(n)}$  and  $g_{ci}^{(n)}$  for  $k = 1, \dots, K$ . In (9), by considering the constraint  $P_i^{(n)} \geq 0$ , we get

$$h_{ii}^{(n)} \geq \frac{NI_{CU,i}^{(n)} + P_{DU,I_{Th}}}{\eta\lambda + \omega_i} \times \left( \nu_i + v - \eta v + f_{ik^*}^{(n)}\mu + \phi_{i,n}h_{ji}^{(n)} \right) \triangleq h_{thres}, \quad (10)$$

i.e., the constraint  $P_i^{(n)} \geq 0$  also imposes a constraint on the required channel gain  $h_{ii}^{(n)}$ , which in turn will have its impact on the integral limits in the expectation over the channel statistics.

Further, in this scenario, the optimal subchannel allocation  $\chi_i^{*(n)}$  of the  $i$ th D2D link should satisfy the following criterion [43]:

$$\chi_i^{*(n)} = \begin{cases} 1, & \varrho^{(n)} \leq H_{in}, \\ 0, & \varrho^{(n)} > H_{in}, \end{cases} \quad (11)$$

where  $\varrho^{(n)}$  is the Lagrange multiplier associated to (3g), and

$$H_{in} = \ln \left( 1 + \frac{\hat{P}_i^{(n)}h_{ii}^{(n)}}{NI_{CU,i}^{(n)} + P_{DU,I_{Th}}} \right) - \frac{\hat{P}_i^{(n)}h_{ii}^{(n)}}{\hat{P}_i^{(n)}h_{ii}^{(n)} + NI_{CU,i}^{(n)} + P_{DU,I_{Th}}} + \phi_{i,n}\hat{P}_j^{(n)}. \quad (12)$$

To find the optimum subchannel allocation (11), we first need to determine the threshold  $H_{in}$ , which depends on the Lagrangian variables through the solution of  $\hat{P}_i^{(n)}$ . To compute the optimal values of the Lagrangian variables, we use the subgradient method:

$$\lambda(t+1) = [\lambda(t) + \alpha_\lambda (\eta(C_0 - SE) - \psi)]^+, \quad (13)$$

$$v(t+1) = [v(t) + \alpha_v ((1 - \eta)(P_{Total} - P_0) - \psi)]^+, \quad (14)$$

$$\nu_i(t+1) = [\nu_i(t) + \alpha_\nu (\bar{\mathbf{P}}(i) - P_{\max}(i))]^+, \quad \forall i \in \{1, 2, \dots, M\}, \quad (15)$$

$$\mu_n(t+1) = [\mu_n(t) + \alpha_\mu (\bar{\mathbf{Q}} - Q_{k^* \max})]^+, \quad (16)$$

$$\omega_i(t+1) = [\omega_i(t) + \alpha_\omega (R_{\min} - R_{DU,i})]^+, \quad (17)$$

$$\phi_{i,n}(t+1) = \left[ \phi_{i,n}(t) + \alpha_\phi \left( \sum_{\substack{j=1 \\ j \neq i}}^M P_j^{(n)} h_{ji}^{(n)} - P_{DU,I_{Th}} \right) \right]^+, \quad (18)$$

where  $\alpha_\lambda, \alpha_v, \alpha_\nu, \alpha_\mu, \alpha_\omega, \alpha_\phi$  are positive gradient-search step-sizes, and  $\lambda(t), v(t), \boldsymbol{\nu}(t), \boldsymbol{\mu}(t), \boldsymbol{\omega}(t)$ , and  $\phi(t)$  are the values of  $\lambda, v, \boldsymbol{\nu}, \boldsymbol{\mu}, \boldsymbol{\omega}$ , and  $\phi$  in iteration  $t$ , respectively. The subgradient algorithm converges to the best value within some range of the optimal value, provided that the step-sizes are sufficiently small [44]–[45].

Now, we restrict our attention to the case of Rician fading channels, and we study the effect of the fading characteristics on the gain of spectrum sharing by evaluating  $R_{DU}$  and  $\bar{\mathbf{P}}(i) = \sum_{n=1}^N \chi_i^{(n)} \mathbb{E}[P_i^{(n)}]$  under Rician fading.<sup>5</sup> Furthermore, we assume that  $f_{ik^*}^{(n)}, h_{ii}^{(n)}$ , and  $g_{ci}^{(n)}$  have non-unit means and are mutually independent, and each channel follows a Rician fading distribution with different variances. The PDF of the channel power gain  $X$  with mean  $\Omega$  (i.e.,  $\Omega = \mathbb{E}[X]$ ) is given by

$$f_X(x) = \frac{(1+J)e^{-J}}{\Omega} \times \exp\left(-\frac{(1+J)x}{\Omega}\right) I_0\left(2\sqrt{J}\sqrt{\frac{1+J}{\Omega}}x\right), \quad (19)$$

where  $J$  is the Rician factor and  $I_0(2\sqrt{x})$  is the modified Bessel function of the first kind and zeroth order. The scattered component of  $f_X(x)$  is modeled as a Gaussian random variable with variance  $1/2$ , thus  $\Omega = 1 + J$  [25].

In the case of a Rician fading channel, the expression for SE from (3b) can be modified as follows:

$$\begin{aligned} SE &= \sum_{i=1}^M \sum_{n=1}^N \chi_i^{(n)} \int_0^\infty \int_0^\infty \int_0^\infty \int_{h_{thres}}^\infty \\ &\times \frac{(1+J_1)(1+J_2)(1+J_3)(1+J_4)e^{-J_1-J_2-J_3-J_4}}{\Omega_{h_{ii}}^{(n)}\Omega_{g_{ci}}^{(n)}\Omega_{f_{ik^*}}^{(n)}\Omega_{h_{ji}}^{(n)}} \\ &\times \ln\left(\frac{h_{ii}^{(n)}}{h_{thres}}\right) \exp\left(-\frac{h_{ii}^{(n)}(1+J_1)}{\Omega_{h_{ii}}^{(n)}} - \frac{g_{ci}^{(n)}(1+J_2)}{\Omega_{g_{ci}}^{(n)}}\right) \\ &\times \frac{h_{ji}^{(n)}(1+J_3) - f_{ik^*}^{(n)}(1+J_4)}{\Omega_{h_{ji}}^{(n)}\Omega_{f_{ik^*}}^{(n)}} I_0\left(2\sqrt{J_1}\sqrt{\frac{1+J_1}{\Omega_{h_{ii}}^{(n)}}}h_{ii}^{(n)}\right) \\ &\times I_0\left(2\sqrt{J_2}\sqrt{\frac{1+J_2}{\Omega_{g_{ci}}^{(n)}}}g_{ci}^{(n)}\right) I_0\left(2\sqrt{J_3}\sqrt{\frac{1+J_3}{\Omega_{f_{ik^*}}^{(n)}}}f_{ik^*}^{(n)}\right) \\ &\times I_0\left(2\sqrt{J_4}\sqrt{\frac{1+J_4}{\Omega_{h_{ji}}^{(n)}}}h_{ji}^{(n)}\right) dh_{ii}^{(n)} dg_{ci}^{(n)} dh_{ji}^{(n)} df_{ik^*}^{(n)}. \quad (20) \end{aligned}$$

<sup>5</sup>Rician fading is commonly used to model propagation paths consisting of one strong direct line-of-sight component and many weaker random components.

Similarly, for the Rician fading channel, the expression  $\bar{\mathbf{P}}(i) = \sum_{n=1}^N \chi_i^{(n)} \mathbb{E}[P_i^{(n)}]$  can be expressed as

$$\begin{aligned} \mathbf{P}(i) &= \sum_{n=1}^N \chi_i^{(n)} \int_0^\infty \int_0^\infty \int_0^\infty \int_{h_{thres}}^\infty \frac{NI_{CU,i}^{(n)} + P_{DU,I_m}}{\Omega_{h_{ii}}^{(n)} \Omega_{h_{ji}}^{(n)} \Omega_{g_{ci}}^{(n)} \Omega_{f_{ik^*}}^{(n)}} \\ &\times \left( \frac{1}{h_{thres}} - \frac{1}{h_{ii}^{(n)}} \right) (1 + J_1)(1 + J_2)(1 + J_3)(1 + J_4) \\ &\times e^{-J_1 - J_2 - J_3 - J_4} \times \exp \left( -\frac{h_{ii}^{(n)}(1 + J_1)}{\Omega_{h_{ii}}^{(n)}} - \frac{g_{ci}^{(n)}(1 + J_2)}{\Omega_{g_{ci}}^{(n)}} \right. \\ &\left. - \frac{h_{ji}^{(n)}(1 + J_3)}{\Omega_{h_{ji}}^{(n)}} - \frac{f_{ik^*}^{(n)}(1 + J_4)}{\Omega_{f_{ik^*}}^{(n)}} \right) I_0 \left( 2\sqrt{J_1} \sqrt{\frac{1 + J_1}{\Omega_{h_{ii}}^{(n)}} h_{ii}^{(n)}} \right) \\ &\times I_0 \left( 2\sqrt{J_2} \sqrt{\frac{1 + J_2}{\Omega_{g_{ci}}^{(n)}} g_{ci}^{(n)}} \right) I_0 \left( 2\sqrt{J_3} \sqrt{\frac{1 + J_3}{\Omega_{h_{ji}}^{(n)}} h_{ji}^{(n)}} \right) \\ &\times I_0 \left( 2\sqrt{J_4} \sqrt{\frac{1 + J_4}{\Omega_{f_{ik^*}}^{(n)}} f_{ik^*}^{(n)}} \right) dh_{ii}^{(n)} dg_{ci}^{(n)} dh_{ji}^{(n)} df_{ik^*}^{(n)}. \quad (21) \end{aligned}$$

*Proposition 1:* For general values of  $K$ , closed-form expressions for (20) and (21) do not exist and (20) and (21) need to be calculated numerically. However, closed-form results can be obtained for  $K = 1$  and  $J = 0$ .

*Proof:* Please see Appendix A. ■

Finally, the maximum ergodic sum rate (SE) and EE of the D2D links can be obtained using (20) and (21), respectively. For  $P_{DU,i}^{(n)} = 0 \forall i$ , i.e., the sparsely deployed scenario, this simplified model was for example used to design a simple power allocation in [31], [40]. In the numerical results section, we will study the tradeoff between EE and SE, and compare the results for the sparsely deployed scenario with the more general scenario with  $P_{DU,i}^{(n)} \neq 0 \forall i$ .

## V. OPTIMIZATION PROBLEM FOR A GENERAL CASE (DENSELY DEPLOYED SCENARIO)

In urban scenarios with medium or high user density, the mutual interference between D2D links in different cells cannot be ignored. In this general case, which we call the densely deployed scenario, a closed-form expression for the power allocation is not obtainable, in contrast to the case with limited interference, as discussed in the previous section.

To find the resource allocation, we consider an iterative procedure, where in each iteration, we first update the subchannel assignment  $\chi_i^{(n)}[t]$  and then compute the power allocation  $P_i^{(n)}[t]$ . The subchannel allocation  $\chi_i^{(n)}[t]$  is determined based on the power allocation  $P_i^{(n)}[t-1]$  in the previous iteration:

$$\chi_i^{(n)}[t] = \begin{cases} 1, & \text{if } i = \arg \max_i \mathbb{E}[\ln(1 + \text{SINR}_i^{(n)}[t-1])], \\ 0, & \text{otherwise.} \end{cases} \quad (22)$$

where  $\text{SINR}_i^{(n)}[t-1]$  is computed using (1). To initialize the iterative algorithm, i.e., to find  $\chi_i^{(n)}[0]$ , we start with the closed-form expression (9).

In each iteration, we need to determine the optimal power allocation  $P_i^{(n)}[t]$  based on the subchannel allocation  $\chi_i^{(n)}[t]$ . However, finding the optimal power allocation is a non-convex problem. As in non-convex problems, the simple approach of using the dual problem is not suitable due to the non-zero duality gap [47], we apply the successive convex approximation method to the problem at hand. In this method, instead of dealing with the highly non-concave rate function terms in (6b)–(6c), we employ a technique based on “difference of two convex functions/sets” (DC) programming<sup>6</sup> [48], [54]. This converts the non-convex function into the difference of two convex functions and the discounted term is approximated by its first order Taylor series. Applying this method to the optimization problem, the non-convex sum rate function included in (6b) is expressed in DC form as:

$$f_i(\mathbf{P}) - q_i(\mathbf{P}), \quad (23)$$

where  $f_i(\mathbf{P})$  and  $q_i(\mathbf{P})$  for  $\forall i \in \{1, 2, \dots, M\}$  are two concave functions defined as

$$f_i(\mathbf{P}) = \sum_{n=1}^N \left[ \ln \left( NI_{CU,i}^{(n)} + \sum_{j=1}^M P_j^{(n)} h_{ji}^{(n)} \right) \right], \quad (24)$$

$$q_i(\mathbf{P}) = \sum_{n=1}^N \left[ \ln \left( NI_i^{(n)} \right) \right]. \quad (25)$$

To convexify the sum rate function (23), we apply the first order approximation of (25) at point  $\mathbf{P}^{(t)}$ :

$$q_i(\mathbf{P}) \approx q_i(\mathbf{P}^{(t)}) + \langle \nabla q_i(\mathbf{P}^{(t)}), (\mathbf{P} - \mathbf{P}^{(t)}) \rangle, \quad (26)$$

where  $\langle \mathbf{X}, \mathbf{Y} \rangle$  denotes the standard inner product on  $\mathbb{R}^{M \times N}$  and  $\mathbf{P}^{(t)}$  is the power allocation matrix at iteration  $t$ . The gradient  $\nabla q_i(\mathbf{P}^{(t)})$  is given by

$$\nabla q_i(\mathbf{P}) = \frac{\partial q_i(\mathbf{P})}{\partial P_j^{(n)}} = \left[ \frac{h_{ji}^{(n)}}{NI_i^{(n)}} \right]. \quad (27)$$

Combining (23)–(27), the sum rate function  $R_{DU,i}$  is approximated by the following concave function with respect to  $\mathbf{P}$ :

$$f_i(\mathbf{P}) - q_i(\mathbf{P}^{(t)}) - \langle \nabla q_i(\mathbf{P}^{(t)}), (\mathbf{P} - \mathbf{P}^{(t)}) \rangle. \quad (28)$$

By using this approximation, we can change (6) into a sequence of convex optimization subproblems [49], where the optimal solution  $\mathbf{P}^{(t)}$  and  $\psi^t$  at iteration  $t > 0$  is obtained by solving the

<sup>6</sup>Note that in this paper, we actually approximate the non-convex function by a difference of two concave functions. However, as maximizing a convex function  $f(x)$  is equivalent with minimizing the concave function  $-f(x)$ , we use in this paper the terminology “convex.”

following convex optimization program:

$$\min_{\mathbf{P}, \psi^t} \psi^t \quad (29a)$$

$$\text{s.t.: } \eta \left( C_0 - \sum_{i=1}^M \mathbb{E} \left[ \left( f_i(\mathbf{P}) - q_i(\mathbf{P}^{(t-1)}) - \langle \nabla q_i(\mathbf{P}^{(t-1)}), (\mathbf{P} - \mathbf{P}^{(t-1)}) \rangle \right) \right] \right) - \psi \leq 0, \quad (29b)$$

$$(1 - \eta) (\mathbf{P}_{\text{Total}} - P_0) - \psi \leq 0, \quad (29c)$$

$$\mathbb{E} \left[ \left( f_i(\mathbf{P}) - q_i(\mathbf{P}^{(t-1)}) - \langle \nabla q_i(\mathbf{P}^{(t-1)}), (\mathbf{P} - \mathbf{P}^{(t-1)}) \rangle \right) \right] \geq R_{\min}, \quad (29d)$$

(3c), (3d).

From (29), it follows that the DC programming generates a sequence of solutions  $\mathbf{P}^{(t)}$ , where in iteration  $t$ , the optimization depends on the solution of the previous iteration  $t - 1$  only. The convexified function  $\sum_{i=1}^M [f_i(\mathbf{P}^{(t)}) - q_i(\mathbf{P}^{(t)})]$  in the different iterations is increasing and converges to a locally optimal solution. In general, DC programming obtains a close to optimal solution [48].

Let us take a closer look at the computational complexity of the optimization problem (29). The main computational cost is related to the computation of  $\mathbb{E}[f_i(\mathbf{P})]$ , which requires at least  $M \times N$  nested numerical integrations because of the  $M \times N$  random variables appearing in the argument of the ln-function inside the expectation (24). To reduce the complexity, we rewrite (24) using Frullani's integral [50, p. 6], i.e.,

$$\ln(1+x) = \int_0^\infty (1 - e^{-sx}) \frac{e^{-s}}{s} ds. \quad (30)$$

By applying (30), the expression  $\mathbb{E}[f_i(\mathbf{P})]$  can be written as

$$\mathbb{E}[f_i(\mathbf{P})] = \sum_{n=1}^N \left( \int_0^\infty \left( 1 - \mathbb{E} \left[ e^{-\frac{z}{N_0 B} P_{C_{U,i}}^{(n)}} \right] \right) \times \mathbb{E} \left[ e^{-\frac{z}{N_0 B} \sum_{j=1}^M P_j^{(n)} h_{ji}^{(n)}} \right] \right) \frac{e^{-z}}{z} dz + \ln(N_0 B), \quad (31)$$

which is equivalent to

$$\mathbb{E}[f_i(\mathbf{P})] = \sum_{n=1}^N \left( \int_0^\infty \left( 1 - \mathbb{E} \left[ \prod_{c=1}^C e^{-\frac{z}{N_0 B} \rho_c^{(n)} g_{ci}^{(n)}} \right] \right) \times \mathbb{E} \left[ \prod_{j=1}^M e^{-\frac{z}{N_0 B} P_j^{(n)} h_{ji}^{(n)}} \right] \right) \frac{e^{-z}}{z} dz + \ln(N_0 B). \quad (32)$$

Using the fact that  $g_{ci}^{(n)}$ ,  $\forall c$ , and also  $h_{ji}^{(n)}$ ,  $\forall j$ , are mutually independent, the expression in (32) becomes:

$$\mathbb{E}[f_i(\mathbf{P})] = \sum_{n=1}^N \left( \int_0^\infty \left( 1 - \prod_{c=1}^C \mathbb{E} \left[ e^{-\frac{z}{N_0 B} \rho_c^{(n)} g_{ci}^{(n)}} \right] \right) \times \prod_{j=1}^M \mathbb{E} \left[ e^{-\frac{z}{N_0 B} P_j^{(n)} h_{ji}^{(n)}} \right] \right) \frac{e^{-z}}{z} dz + \ln(N_0 B). \quad (33)$$

Now, we focus on evaluating  $\mathbb{E} \left[ e^{-\frac{z}{N_0 B} \rho_c^{(n)} g_{ci}^{(n)}} \right]$ . Since  $g_{ci}^{(n)}$  is modeled by the Rician distribution from (19) and upon invoking [46], we have

$$\begin{aligned} & \mathbb{E} \left[ e^{-\frac{z}{N_0 B} \rho_c^{(n)} g_{ci}^{(n)}} \right] \\ &= \frac{(1+J)e^{-J}}{\Omega_{g_{ci}}^{(n)}} \int_0^\infty e^{-\frac{z}{N_0 B} \rho_c^{(n)} g_{ci}^{(n)}} e^{-\frac{(1+J)g_{ci}^{(n)}}{\Omega_{g_{ci}}^{(n)}}} \\ & I_0 \left( 2\sqrt{J} \sqrt{\frac{1+J}{\Omega_{g_{ci}}^{(n)}} g_{ci}^{(n)}} \right) dg_{ci}^{(n)} = \frac{N_0 B(1+J)}{N_0 B(1+J) + \rho_c^{(n)} z \Omega_{g_{ci}}^{(n)}} \\ & \times e^{-\frac{J z \rho_c^{(n)} \Omega_{g_{ci}}^{(n)}}{N_0 B(1+J) + z \rho_c^{(n)} \Omega_{g_{ci}}^{(n)}}}. \end{aligned} \quad (34)$$

Then, we can compute  $\mathbb{E} \left[ e^{-\frac{z}{N_0 B} P_j^{(n)} h_{ji}^{(n)}} \right]$  in a similar manner as (34). As a result, the expression (33) can be simplified to a single integration

$$\begin{aligned} \mathbb{E}[f_i(\mathbf{P})] &= \sum_{n=1}^N \left( \int_0^\infty \left( 1 - \prod_{c=1}^C \right. \right. \\ & \left. \left. \times \frac{N_0 B(1+J)}{N_0 B(1+J) + \rho_c^{(n)} z \Omega_{g_{ci}}^{(n)}} e^{-\frac{J z \rho_c^{(n)} \Omega_{g_{ci}}^{(n)}}{N_0 B(1+J) + z \rho_c^{(n)} \Omega_{g_{ci}}^{(n)}}} \right. \right. \\ & \left. \left. \times \prod_{j=1}^M \frac{N_0 B(1+J)}{N_0 B(1+J) + P_j^{(n)} z \Omega_{h_{ji}^{(n)}}} e^{-\frac{J z P_j^{(n)} \Omega_{h_{ji}^{(n)}}}{N_0 B(1+J) + z P_j^{(n)} \Omega_{h_{ji}^{(n)}}} \right) \right) \\ & \times \frac{e^{-z}}{z} dz + \ln(N_0 B) \end{aligned} \quad (35)$$

After substituting (35) into the main problem (29), we can formulate the Lagrangian dual problem in each iteration and then the optimal power allocation can be obtained using the steepest gradient descent method. Specifically, the Lagrangian for the optimization problem (29) becomes (36), shown at the bottom of the next page, where  $\lambda$ ,  $\nu$ ,  $\boldsymbol{\nu} = (\nu_1, \nu_2, \dots, \nu_M)$ ,  $\boldsymbol{\mu}$  and  $\boldsymbol{\omega}$  are (vectors of) Lagrangian dual variables.

The Lagrangian dual problem as an unconstrained maximization can be solved in an iterative way by the steepest gradient descent method

$$x(\tau+1) = x(\tau) - \beta \left( \frac{\partial}{\partial x} L(P_i, \lambda, \nu, \boldsymbol{\mu}, \boldsymbol{\omega}) \right), \quad (37)$$

where  $x(\tau)$  is the value of  $x$  at iteration  $\tau$  and  $\beta$  is the step size, and  $x \in \{P_i^{(n)}, \lambda, \nu, \boldsymbol{\mu}, \boldsymbol{\omega}\}$  in order to find the optimum power allocation.

To end this section, our iterative algorithm under the densely deployed scenario, that jointly allocates subchannels and power in our system model, is summarized in Algorithm 1. This algorithm starts with obtaining a feasible solution for the subchannel (11) and transmit power (9) allocation from the sparsely deployed scenario. In each iteration, the algorithm alternatively assigns subchannels and allocates power to D2D users. The iterations continue until no further improvement is made. The proposed DC programming as well as MOOP optimization

---

**Algorithm 1:** Proposed Iterative Subchannel and Power Allocation Algorithm Based on MOOP and DC Programming.

---

- 1: **Input:** Initialize  $t = 0$ ,  $t = T_{\max}$ , set appropriate weighting factor  $\eta$
  - 2: Calculate  $\mathbf{P}[0]$  and  $\chi[0]$  using the solution of (9) and (11), respectively.
  - 3: **Repeat.**
  - 4: Compute the subchannel allocation  $\chi[t]$  using (22) with  $\mathbf{P}[t - 1]$
  - 5: Compute the transmit power  $\mathbf{P}[t]$  using (29) with  $\chi[t]$ . and store intermediate resource allocation  $\mathbf{P}[t]$
  - 6: Set  $t = t + 1$  and  $\mathbf{P}[t] = \mathbf{P}$
  - 7: **Until convergence** or  $t = T_{\max}$
  - 8: **Output:**  $\chi^* = \chi[t]$ ,  $\mathbf{P}^* = \mathbf{P}[t]$
  - 9: **End**
- 

based resource allocation algorithm provides a sub-optimal solution in a finite number of iterations from both a joint optimization as well as power allocation point of view. In the following, we propose an optimal power allocation based on the sequential fractional programming [53] resource allocation algorithm, which has a polynomial time computational complexity to find a compromise between the complexity and performance of the proposed scheme.

## VI. POWER ALLOCATION SOLUTION: SEQUENTIAL FRACTIONAL PROGRAMMING

The proposed framework based on the MOOP optimization for the resource allocation algorithm provides a systematic procedure to achieve suboptimal solutions with a lower complexity. However, it is desirable to provide a solution for benchmarking, which is often difficult without the knowledge of the true optimal point. In the following, we propose an close-to-optimal method for the power allocation having a

higher complexity than that of the suboptimal solution proposed in Section V. In this section, we aim at finding an optimal power allocation policy for the given subchannel assignment based on the equation (22) to strike a balance between EE and SE for D2D users. First, we transform problem (3) to a mathematically tractable problem as follows

$$\begin{aligned} \max_{\mathbf{P}} \quad & \text{EE} = \frac{\text{SE}}{\sum_{i=1}^M \sum_{n=1}^N \epsilon_i \chi_i^{(n)} \mathbb{E}[P_i^{(n)}] + \sum_{i=1}^M P_{C_i}} \\ \text{s.t.} \quad & (3c)-(3g). \end{aligned} \quad (38)$$

In order to solve the optimization problem (38), we employ fractional programming, which is combined with the sequential optimization points fulfilling the Karush-Kuhn-Tucker (KKT) first order optimality condition of the EE maximization. It is worth mentioning that the sequential fractional programming approach actually obtains global optimality [53]. Now, we rewrite the numerator of the objective function (38), which is not a concave function in general, as the difference of concave functions

$$\begin{aligned} \max_{\mathbf{P}} \quad & \text{EE} = \frac{\sum_{i=1}^M \mathbb{E}[f_i(\mathbf{P}) - q_i(\mathbf{P})]}{\sum_{i=1}^M \sum_{n=1}^N \epsilon_i \chi_i^{(n)} \mathbb{E}[P_i^{(n)}] + \sum_{i=1}^M P_{C_i}} \\ \text{s.t.} \quad & (3c)-(3g), \mathbb{E}[f_i(\mathbf{P}) - q_i(\mathbf{P})] \geq R_{\min}. \end{aligned} \quad (39)$$

To find a convex approximation for the rate function, we employ the first order Taylor approximation of  $q_i(\mathbf{P})$  at point  $\mathbf{P}^{(t)}$  as in (39). After the convexification of the rate function, the problem reduces to

$$\begin{aligned} \max_{\mathbf{P}} \quad & \frac{\sum_{i=1}^M \mathbb{E}[f_i(\mathbf{P}) - q_i(\mathbf{P}^{(t)}) - \langle \nabla q_i(\mathbf{P}^{(t)}), (\mathbf{P} - \mathbf{P}^{(t)}) \rangle]}{\sum_{i=1}^M \sum_{n=1}^N \epsilon_i \chi_i^{(n)} \mathbb{E}[P_i^{(n)}] + \sum_{i=1}^M P_{C_i}} \\ \text{s.t.} \quad & \mathbb{E}[(f_i(\mathbf{P}) - q_i(\mathbf{P}^{(t-1)}) - \langle \nabla q_i(\mathbf{P}^{(t-1)}), (\mathbf{P} - \mathbf{P}^{(t-1)}) \rangle)] \geq R_{\min}, \\ & (3c)-(3g). \end{aligned} \quad (40)$$

$$\begin{aligned} L(P_i, \lambda, v, \nu, \xi^{(n)}, \omega) = & \psi^t + \lambda \\ & \times \left[ \eta \left( C_0 - \left( \sum_{i=1}^M \sum_{n=1}^N \left( \int_0^\infty \left\{ 1 - \left[ \prod_{c=1}^C \frac{N_0 B(1+J)}{N_0 B(1+J) + \rho_c^{(n)} z \Omega_{g_{ci}}^{(n)}} e^{-\frac{J z \rho_c^{(n)} \Omega_{g_{ci}}^{(n)}}}{N_0 B(1+J) + z \rho_c^{(n)} \Omega_{g_{ci}}^{(n)}} dg_{ci}^{(n)} \right\} \right) \right) \right) \right. \\ & \times \left. \left[ \prod_{j=1}^M \frac{N_0 B(1+J)}{N_0 B(1+J) + P_j^{(n)} z \Omega_{h_{ji}}^{(n)}} e^{-\frac{J z P_j^{(n)} \Omega_{h_{ji}}^{(n)}}{N_0 B(1+J) + z P_j^{(n)} \Omega_{h_{ji}}^{(n)}}} \right] \frac{e^{-z}}{z} dz \right] \Big) \\ & + \ln(N_0 B) - \sum_{i=1}^M \mathbb{E} \left[ \left( q_i(\mathbf{P}^{(t)}) + \langle \nabla q_i(\mathbf{P}^{(t)}), (\mathbf{P} - \mathbf{P}^{(t)}) \rangle \right) \right] \Big) - \psi \Big] + v((1 - \eta)(P_{\text{Total}} - P_0) - \psi) \\ & + \nu_i \sum_{n=1}^N \left( \mathbb{E}[P_i^{(n)}] - P_{\max}(i) \right) + \mu(\bar{\mathbf{Q}} - \mathbf{Q}_{k^* \max}) \\ & + \omega_i \left( R_{\min} - \sum_{n=1}^N \mathbb{E} \left[ \left( f_i(\mathbf{P}) - q_i(\mathbf{P}^{(t-1)}) - \langle \nabla q_i(\mathbf{P}^{(t-1)}), (\mathbf{P} - \mathbf{P}^{(t-1)}) \rangle \right) \right] \right) \end{aligned} \quad (36)$$

The optimization problem (40) belongs to the class of fractional programming, which can be globally solved by means of fractional programming theory [53]. Therefore, we adopt an iterative approach known as Dinkelbach's algorithm [52], [55]. At iteration  $t_i$ :

$$\begin{aligned} \max_{\mathbf{P}} \quad & \sum_{i=1}^M \mathbb{E} \left[ f_i(\mathbf{P}) - q_i(\mathbf{P}^{(t)}) - \langle \nabla q_i(\mathbf{P}^{(t)}), (\mathbf{P} - \mathbf{P}^{(t)}) \rangle \right] \\ & - \lambda_{t_i} \left( \mathbf{P}_{\text{Total}}(\mathbf{P}) \right) \\ \text{s.t.} \quad & \mathbb{E} \left[ \left( f_i(\mathbf{P}) - q_i(\mathbf{P}^{(t-1)}) - \langle \nabla q_i(\mathbf{P}^{(t-1)}), (\mathbf{P} - \mathbf{P}^{(t-1)}) \rangle \right) \right] \geq R_{\min}, \end{aligned} \quad (41)$$

The power control policy obtains the optimal EE, i.e.,  $\lambda_{t_i}^* = \frac{\text{SE}(\mathbf{P}^*)}{\mathbf{P}_{\text{Total}}(\mathbf{P}^*)}$ , if and only if

$$\begin{aligned} \max_{\mathbf{P}} \quad & \sum_{i=1}^M \mathbb{E} \left[ f_i(\mathbf{P}) - q_i(\mathbf{P}^{(t)}) - \langle \nabla q_i(\mathbf{P}^{(t)}), (\mathbf{P} - \mathbf{P}^{(t)}) \rangle \right] \\ & - \lambda_{t_i}^* \left( \sum_{i=1}^M \sum_{n=1}^N \epsilon_i \chi_i^{(n)} \mathbb{E}[P_i]^{(n)} + \sum_{i=1}^M P_{C_i} \right) \\ = \quad & \sum_{i=1}^M \mathbb{E} \left[ f_i(\mathbf{P}^*) - q_i(\mathbf{P}^*) \right] - \lambda_{t_i}^* \left( \mathbf{P}_{\text{Total}}(\mathbf{P}^*) \right) = 0. \end{aligned} \quad (42)$$

*Theorem 1:* Optimization problem (41) is monotonically increasing and converges to a  $\mathbf{P}^*$  (optimal solution) provided that  $\mathbf{P}^{(t)} = \mathbf{P}^{*(t-1)}$ , which results a globally optimal solution of (42).

*Proof:* The proof is given in Appendix B.  $\blacksquare$

As the problem in (41) is a monotonically increasing convex optimization problem at each iteration, it can be solved efficiently using optimization packages including interior point methods such as CVX. The detailed scheme of the proposed method is provided in Algorithm 2. It is worth mentioning that by fixing the subchannel assignment, Algorithm 2 converges to the maximum energy efficiency optimized with respect to the power allocation variables only.

## VII. COMPUTATIONAL COMPLEXITY

In this section, we aim at investigating the computational complexity of the proposed algorithms for the different scenarios. The complexity of computation for the case with limited interference is  $\mathcal{O}(NM(\frac{1}{\epsilon^2}))$ , where  $\epsilon$  is the threshold value between two consecutive iterations of sub-gradient approach [56]. For the densely deployed scenario, it is obvious that the algorithm proposed in Section V consists of two steps. Assigning the best subchannel for each D2D transmitter is determined from (22) and then, for the chosen subchannel, the optimal power allocation is obtained based on the DC programming using (29). For the optimal subchannel assignment, the order of complexity is  $\mathcal{O}(NM)$ , while for the power allocation, the complexity of computation

---

### Algorithm 2: Iterative Resource Allocation Algorithm Based on Sequential Fractional Programming.

---

- 1: **Input** :  $T_i^{\max}$  = the maximum number of iterations and  $\delta$  = the maximum error tolerance
  - 2: Set  $\lambda_{t_i} = 0$  and iteration index  $t_i = 0$
  - 3: **while**  $\lambda_{t_i} - \lambda_{t_{i-1}} > \delta$  **do**
  - 4: Solve the optimization problem (42) for a given  $\lambda_{t_i}$  to obtain optimal power control  $\mathbf{P}^*$
  - 5: Set  $t_i = t_i + 1$
  - 6: Set  $\lambda_{t_i} = \frac{\text{SE}(\mathbf{P}^*)}{\mathbf{P}_{\text{Total}}(\mathbf{P}^*)}$
  - 7: **end while**
  - 8: **Output**: Set  $\{\mathbf{P}^*\} = \{\mathbf{P}_{t_{i-1}}^*\}$
- 

TABLE II  
COMPLEXITY ORDER OF THE PROPOSED SCENARIOS

Scenario	Order
Case with Limited Interference	$\mathcal{O}(NM(\frac{1}{\epsilon^2}))$
Densely Deployed Algorithm 1:	$\mathcal{O}((NM + NM^3(\frac{1}{\epsilon^2}))\delta)$
Densely Deployed: Algorithm 2	$\mathcal{O}(T_{\text{Dinkelbach}} T_{\text{DC}}(NM)^4) + \mathcal{O}(NM)$

is of order  $\mathcal{O}(NM^3(\frac{1}{\epsilon^2}))$ . Therefore, the total computation complexity for the general scenario is  $\mathcal{O}((NM + NM^3(\frac{1}{\epsilon^2}))\delta)$  where  $\delta$  is the number of iterations required for the proposed suboptimal algorithm. Finally, we obtain the complexity order of sequential fraction programming from Section VI. The optimization problem (41) includes  $NM$  variables and  $2M + N$  linear convex constraints. Hence, the asymptotically computational complexity is of order  $\mathcal{O}(T_{\text{Dinkelbach}} T_{\text{DC}}(NM)^4) + \mathcal{O}(NM)$ , where  $T_{\text{Dinkelbach}}$  and  $T_{\text{DC}}$  are the number of iterations required for reaching convergence in the Dinkelbach and DC methods, respectively [55]. The order of computational complexity of the different methods is summarized in Table II.

## VIII. SIMULATION RESULTS

In this section, we present numerical results for the ergodic EE and SE of D2D communications for the case with limited interference and the densely deployed scenario. We assume a multi-cellular network with  $C = 2$  each with radius 250 m and  $M = 4$  D2D links with maximum distance 30 m. Furthermore, we assume that there are  $N = 8$  subchannels. Without loss of generality, we assume that an equal power allocation is adopted for the cellular users. The rest of the main simulation parameters are given in Table III.

### A. Energy Efficiency Versus Maximum Interference Level Temperature

In this section, we focus on the impact of the interference temperature  $Q_{\max}$  from D2D users to CU on the ergodic EE. We assume that for each of the CUs the interference level is equal, i.e.,  $Q_{k,\max} = Q_{\max}$ . Fig. 1 illustrates the EE versus different levels

TABLE III  
SIMULATION PARAMETERS

Parameter	Value
Cell diameter	250 m
Distance between D2D link	30m
Number of BS ( $C$ )	2
Number of sub-carriers ( $N$ )	8
Noise power	-120 dBm
Sub-carrier bandwidth	180 kHz
Path-loss model for cellular links	$128.1 + 37.6 \log(d)$
Path-loss model for D2D links	$148.1 + 40 \log(d)$
Fading distribution	Rician fading 3 dB
Power amplifier efficiency of the $i$ th D2D user ( $\epsilon_i$ )	20%
Constant power consumed by the $i$ th D2D user ( $P_{C_i}$ )	20 dBm
Maximum transmit power of the cellular	40 dBm
Maximum transmit power of the D2D users	23 dBm
Minimum data rate requirement ( $\bar{R}_{\min}$ )	1 bps/Hz
$P_{DU, I_{Th}}$	-70 dBm
$Q_{\max}$	-60 dBm
$\eta$ for the limited interference scenarios	0.7
$\eta$ for densely deployed scenario	0.4

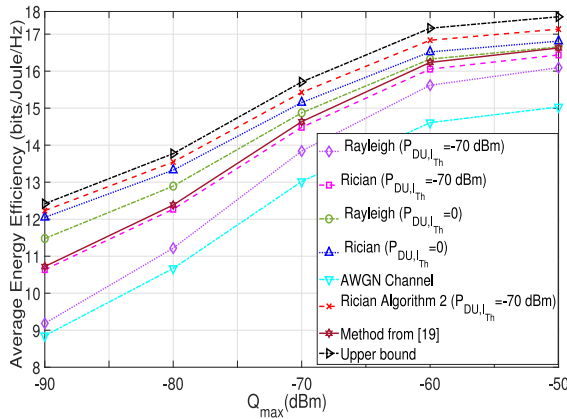


Fig. 1. Average energy efficiency of the D2D users versus the interference temperature limit ( $Q_{\max}$ ) dBm for the limited interference scenario.

of the interference temperature for different types of fading channels in the limited interference scenario. In this figure, we observe that the EE increases when the allowable interference level  $Q_{\max}$  increases and saturates for larger  $Q_{\max}$ . This can be explained as follows. When  $Q_{\max}$  is small, the power allocation is restricted by constraint (3d). By increasing  $Q_{\max}$ , this constraint becomes less stringent implying that we have more degrees of freedom to allocate the power. This results in an improvement of the EE. When  $Q_{\max}$  becomes large, however, the power allocation is no longer restricted by the constraint on  $Q_{\max}$ , but now it is restricted by the maximum average power (3c). As the total power may not exceed  $P_{\max}$ , the power allocation will become independent of  $Q_{\max}$ , resulting in the saturation of the EE. The figure also illustrates the effect of different channel distributions. Note that, if we set  $J = 0$  in (19), the Rician channel reduces to a Rayleigh channel. We observe that the EE of the Rician channel is higher than that of the Rayleigh channel, which in turn is higher than the EE of the AWGN channel. The higher EE of the Rician channel can be explained by the higher SE for a given system power consumption due to the presence of the LoS component facilitating efficient communication. Further, we obtain the higher EE of the Rician and

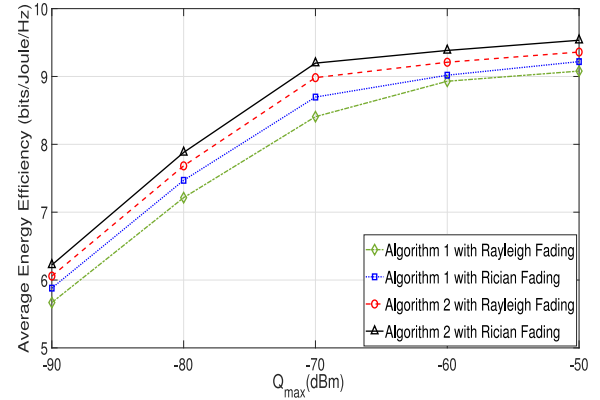


Fig. 2. Average energy efficiency of the D2D users versus the interference temperature limit ( $Q_{\max}$ ) dBm for densely deployed scenario.

Rayleigh channel compared to the AWGN channel. In particular, the D2D network can benefit from opportunistically increasing its transmission power where the interference channel from the D2D users toward the CUs is in deep fading. A similar behavior was observed for the throughput in [51]. Comparing the different scenarios, we see that the average EE for the sparsely deployed scenario with ( $P_{DU, i}^{(n)} = 0$ ) is larger than that of the general limited interference scenario with  $P_{DU, I_{Th}} = -70$  dBm. This is expected as the interference between D2D co-channels can be ignored in the sparse scenario, leading to an enhancement of the SE. For comparison, we also compare the performance of our proposed algorithm with the method in [19]. Although the algorithm in [19] and sparsely deployed scenario have the same system model, our solution reaches a higher EE than that of the method in [19]. For comparison, we also evaluate the EE for the limited interference scenario using Algorithm 2. This algorithm will approximate the close-to-optimal solution closer than Algorithm 1, at the expense of a higher complexity. Furthermore, an upper bound on the EE can be obtained by applying Algorithm 2 to the sparsely deployed scenario. Both results are given in Fig. 1. We observe that applying Algorithm 2 to the limited interference scenario yields 92% of the upper bound performance, while Algorithm 1 only obtain 84% of the upper bound.

Fig. 2 shows the average EE versus interference threshold  $Q_{\max}$  for the densely deployed scenario. We compare the results from Algorithm 1 and Algorithm 2. Similar to the limited interference scenario, the average system EE first increases when  $Q_{\max}$  grows larger. Further, the EE for the Rayleigh fading channel is lower than that for the Rician channel, which is in agreement with the results from Fig. 1. In particular, the Rayleigh fading channel achieves a lower average system EE compared to the Rician fading channel since the LoS link of Rician fading facilitates an efficient communication. Comparing the results of the two algorithms, we see Algorithm 2 has a substantial better performance than that of Algorithm 1 due to obtaining the optimal solution for the power control.

## B. Convergence of Iterative Algorithms

Fig. 3 depicts the average system EE of the proposed iterative algorithms versus the number of iterations for the densely

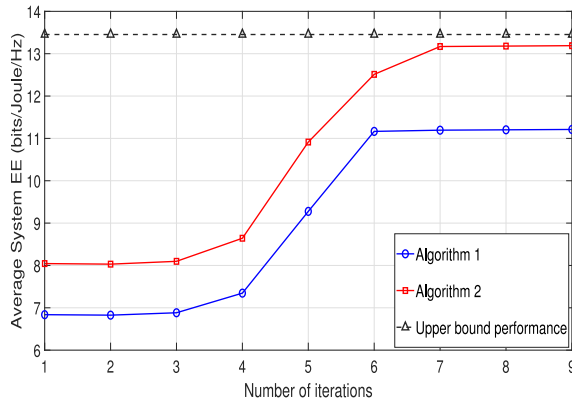


Fig. 3. Average system EE of the D2D users versus the number of iterations for densely deployed scenario.

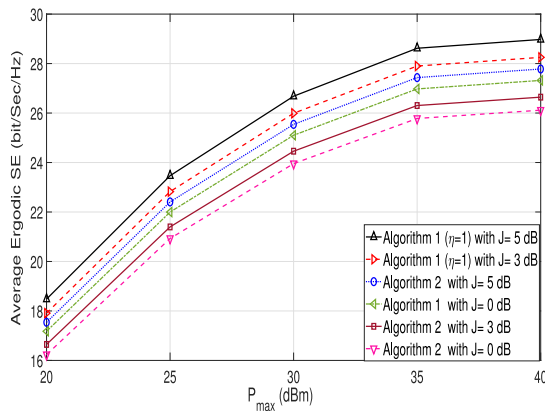


Fig. 4. Average ergodic SE of the D2D users versus the maximum D2D transmit power with Rician fading channel for densely deployed scenario.

deployed scenario in a Rician fading channel. We also plot the upper bound performance of the system to demonstrate the suboptimality of the proposed method. It can be observed from this figure that the iterative algorithm converges to 92% and 84% of the upper bound<sup>7</sup> performance for Algorithm 2 and Algorithm 1, respectively. This figure also demonstrates that even though the speed of convergence differs from one case to another, in both scenarios our algorithm converge after a small number of iterations.

### C. Performance Gain Versus Maximum D2D Transmit Power

In this section, we investigate the average system ergodic SE and average system ergodic EE versus the maximum allowable D2D transmit power  $P_{max}$ .

In Fig. 4, we present the average ergodic SE versus  $P_{max}$ . As can be observed from Fig. 4, the average system ergodic SE for the resource allocation schemes of Algorithm 1 and Algorithm 2, increases monotonically with the maximum D2D transmit power. This is because the received SINR at the D2D users can be improved by optimally allocating the additional available transmit power via the solution of the problem in (3), which leads to an improvement of the system ergodic SE. However,

<sup>7</sup>The upper bound in Fig. 3 is obtained by removing constraints (3d) and (3g) from the optimization problem in (3) for the case of the Rician fading channel.

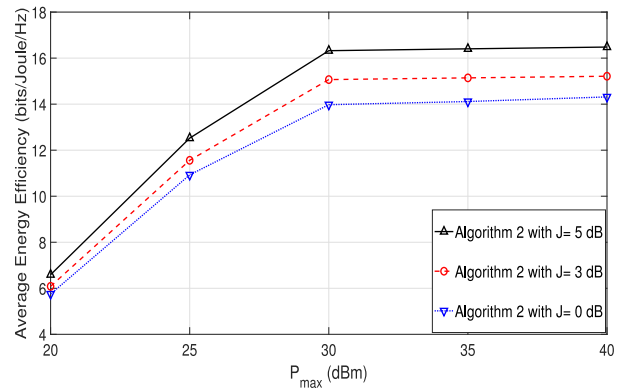


Fig. 5. Average EE of the D2D users versus the maximum D2D transmit power for densely deployed scenario.

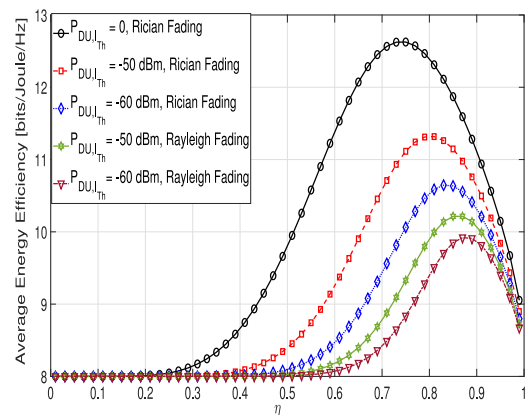


Fig. 6. Energy efficiency vs  $\eta$  for the limited interference scenario.

there is a diminishing return in the average system throughput when  $P_{max}$  is higher than 35 dBm. In fact, as the D2D transmit power increases, the interference power arising from co-channel users becomes more severe, which degrades the received D2D signals. As a result, the throughput of the D2D transmission will decrease. We also observe that Algorithm 1 for weight factor  $\eta = 1$  has a better performance compared to Algorithm 2. This is because for  $\eta = 1$ , Algorithm 1 only focuses on the throughput maximization. In other words, this case ignores power minimization for SE maximization. We also observe that when the Rician factor increases, the system throughput for D2D users increases as well, as the LoS link becomes stronger.

In Fig. 5, we investigate the average ergodic EE versus  $P_{max}$ . It can be observed that the average system EE of the proposed Algorithm 2 is a monotonically non-decreasing function of  $P_{max}$ . In particular, by increasing the value of  $P_{max}$ , the system EE first quickly increases and then saturates when  $P_{max} \geq 30$  dBm since the resource allocator is not willing to consume more power when the maximum EE is obtained.

### D. Average Ergodic EE Versus Different Values of Weight

In this section, we present the average ergodic EE versus different values of weight  $\eta$  for different scenarios.

*Limited Interference Scenario:* Fig. 6 shows the curves of the EE versus  $\eta$  for different values of the interference threshold

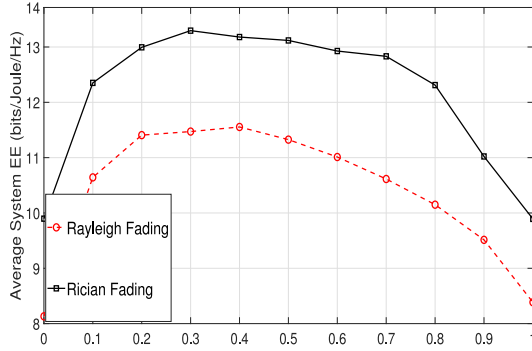


Fig. 7. Average system energy efficiency vs  $\eta$  for densely deployed scenario.

$P_{DU,I_{Th}}$  for the limited interference scenario. The EE plot follows a bell-shaped curve of which the value and position of the maximum is a function of the value of  $P_{DU,I_{Th}}$ . Decreasing  $P_{DU,I_{Th}}$  will result in a reduction of the EE, and the position of the maximum will shift towards larger values of  $\eta$ . The shape of the curve can be explained as follows. When  $\eta$  is small, the EE increases with  $\eta$ , because an increase of  $\eta$  increases the preference given to the rate. In this case, the growth in the SE is more significant than the increase of the total power consumption  $P_{Total}$ , making the EE ratio increase. When  $\eta$  increases towards 1, the increase in the power will dominate the increase in the ergodic SE, causing a decrease of the EE.

*Densely Deployed Scenario:* Fig. 7 shows the EE against the weighting factor  $\eta$  for varying fading channels for a densely deployed scenario. As expected, this figure illustrates that the EE is higher for a Rician channel compared to a Rayleigh channel, which is expected as the LoS link facilitates the communication. Furthermore, by increasing  $\eta$ , the EE first increases and then decreases until it achieves its minimum value. As can be seen from this figure, we observe that the peak value of EE occurs at a lower value of  $\eta$ . The shape of the curve can be explained as follows. When  $\eta$  is small, the EE increases with  $\eta$ , because an increase of  $\eta$  increases the preference given to the rate gain. In this case, the growth in the sum rate is more significant than the increase of the total power consumption making the EE ratio increase. When  $\eta$  increases towards 1, the increase in the power consumption will dominate the system performance, the gain in ergodic sum-rate results in a decrease of the EE. Note that by comparing Fig. 6 and Fig. 7, it can be concluded that the value of  $\eta$  has a large effect on the obtainable EE in the considered scenarios. For example, in the limited interference scenario, the SINR will be larger than in the densely deployed scenario for a given transmit power. As a consequence, the limited interference scenario will achieve higher data rate, and the weight factor  $\eta$  for which the maximum EE is attained, leans toward higher values.

### E. Tradeoff Between EE and SE

*Limited Interference Scenario:* The results displayed in Fig. 8 represent the tradeoff between EE and SE for different values of fading channels, by changing the weighting coefficient  $\eta$  from 0 to 1. This figure, which follows a bell-shaped curve, shows that when the ergodic SE increases, the EE first increases very

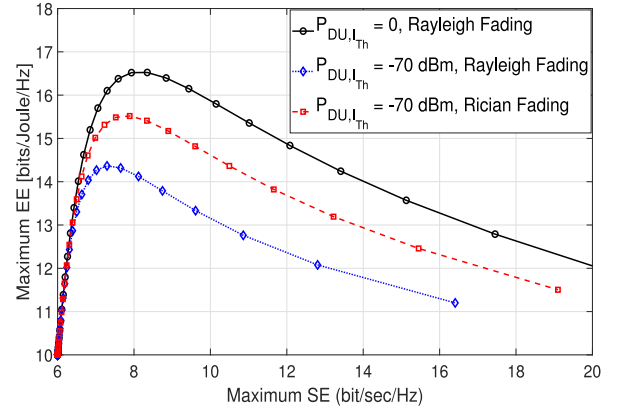


Fig. 8. Tradeoff between EE and SE for limited interference scenario.

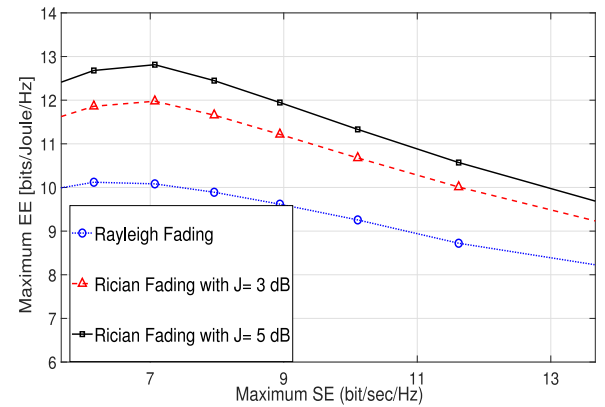


Fig. 9. Tradeoff between EE and SE for densely deployed scenario.

sharply to reach a maximum and then starts to decrease. This can be explained as follows. To achieve higher values of SE, the D2D user needs to transmit more power. However, the gain in SE (in the numerator of the EE) by increasing the power is smaller than the increase of the power (in the denominator of the EE), leading to this reduction of the EE. Another interesting observation is that the maximum value of the EE depends on the Rician factor i.e., higher  $J$  will result in higher EE. The reason for this trend is that when  $J$  increases, the stronger LoS significantly improves the performance of communication links.

*Densely deployed scenario:* In Fig. 9, the behavior of the maximum EE versus the maximum ergodic SE is studied for different fading channels. This figure shows the tradeoff between EE and ergodic SE in densely deployed networks. Similar to the limited interference scenario, the maximum value of the EE depends on the Rician factor  $J$ . This observation can be explained that by increasing the Rician factor, the data rate increases while consuming less power due to having good channel quality.

Fig. 10 illustrates the average ergodic SE versus the average total power for Rician and Rayleigh fading channels for the densely deployed scenario. As can be seen from this figure, when the value of the transmission power increases, the value of the SE increases as well. The figure also shows that the maximized SE for the Rician fading channels is consistently higher than for

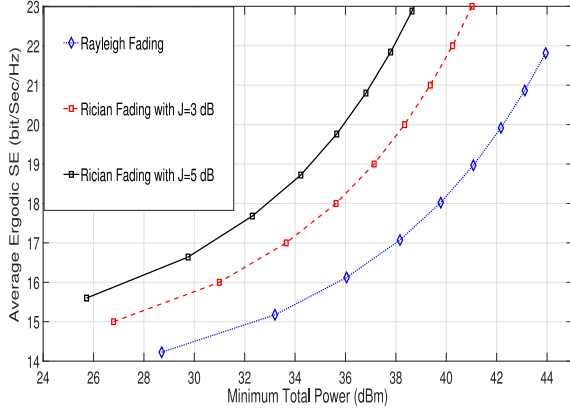


Fig. 10. Average Ergodic SE versus total minimum power for densely deployed scenario.

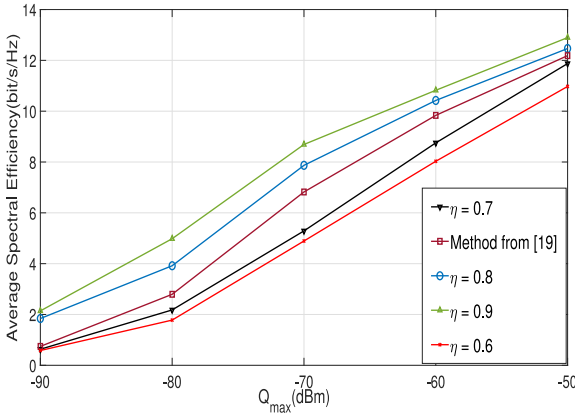


Fig. 11. spectral efficiency of the D2D users versus the interference temperature limit ( $Q_{\max}$ ) dBm for the limited interference scenario.

Rayleigh fading channels. We also observe that due to having LoS communication, the quality of the communication link significantly improves and the users are able to achieve a higher data rate for the same transmit power.

In Fig. 11, the ergodic SE versus  $Q_{\max}$  is shown for different values of  $\eta$  when the minimum required energy efficiency is 4 (bits/Joule/Hz). In this figure, we also compare the results obtained from the proposed solution in the limited interference scenario and the solution in [19] for the sake of fair comparison. As can be seen, for  $\eta = 0.6$ , the SE in [19] is slightly better than that of our solution, however this trend is reversed for  $\eta \geq 0.8$ . The reason is straightforward as the SE totally depends on the value of  $\eta$ . In fact, when more weight is given to the SE, this value of  $\eta$  results in a higher SE. Hence, the balancing parameter  $\eta$  allows us to balance SE and EE.

## IX. CONCLUSION

In this paper, we investigated the tradeoff between ergodic EE and SE for mobile D2D communication as an underlay to cellular networks for two different types of practical D2D communication models, namely a limited interference and a

densely deployed scenario. In particular, we obtained the maximum joint EE and ergodic sum rate of the D2D network for the two scenarios by formulating a MOOP that maximizes the ergodic sum rate and simultaneously minimizes the total transmit power of D2D users. This MOOP is constrained for an average received interference power at the CUs and a transmit power at each D2D user. Besides, an optimal power allocation based on the sequential fractional programming algorithm with polynomial time computational complexity was developed. The computational complexity of the given methods is discussed. Our results showed a tradeoff between the achievable EE and ergodic sum rate, where the maximum EE occurs for small values of the rate and then the EE decreases when the rate is increased. Another interesting point from the simulation results is that the performance of the system under Rician fading channels is always higher than that under Rayleigh fading channel as the LoS link facilitates efficient communication.

## APPENDIX

### A. CLOSED-FORM EXPRESSIONS FOR SE AND $\bar{\mathbf{P}}(i)$

Here, we derive the closed-form expressions for SE and  $\bar{\mathbf{P}}(i)$  from (20) and (21) when  $K = 1$  and  $J = 0$ . Upon invoking [46], (20) transforms into

$$\begin{aligned}
 \text{SE} = & \sum_{i=1}^M \sum_{n=1}^N \chi_i^{(n)} \frac{1}{\mu_n \Omega_{f_{ik^*}}^{(n)} - \phi_{i,n} \Omega_{h_{ji}}} \left( e^{\frac{l_1^{(n)}}{\mu_n \Omega_{f_{ik^*}}^{(n)}}} \mu_n \Omega_{f_{ik^*}}^{(n)} \right. \\
 & \times q_{i,1}^{(n)} + (-\mu_n \Omega_{f_{ik^*}}^{(n)} + \phi_{i,n} \Omega_{h_{ji}}) \text{Ei} \left( -\frac{l_1^{(n)} (N_0 + P_{DU, I_{\text{Th}}})}{l_2^{(n)} \Omega_{h_{ii}}^{(n)}} \right) \\
 & + e^{\frac{N_0 + P_{DU, I_{\text{Th}}}}{\rho_c^{(n)} \Omega_{g_{ci}}^{(n)}}} \mu_n \Omega_{f_{ik^*}}^{(n)} q_{i,2}^{(n)} - e^{\frac{N_0 + P_{DU, I_{\text{Th}}}}{\rho_c^{(n)} \Omega_{g_{ci}}^{(n)}}} \phi_{i,n} \Omega_{h_{ji}} q_{i,2}^{(n)} \\
 & - e^{\frac{\mu_n (N_0 + P_{DU, I_{\text{Th}}}) \Omega_{f_{ik^*}}^{(n)} + l_1^{(n)} \rho_c^{(n)} \Omega_{g_{ci}}^{(n)} + l_2^{(n)} \Omega_{h_{ii}}^{(n)}}{\mu_n \Omega_{f_{ik^*}}^{(n)} \rho_c^{(n)} \Omega_{g_{ci}}^{(n)}}} \mu_n \Omega_{f_{ik^*}}^{(n)} q_{i,3}^{(n)} \\
 & + e^{\frac{l_1^{(n)}}{\phi_{i,n} \Omega_{h_{ji}}^{(n)}}} \phi_{i,n} \Omega_{h_{ji}} \text{Ei} \left( -\frac{l_1^{(n)} (N_0 + P_{DU, I_{\text{Th}}})}{l_2^{(n)} \Omega_{h_{ii}}^{(n)}} - \frac{l_1^{(n)}}{\phi_{i,n} \Omega_{h_{ji}}^{(n)}} \right) \\
 & \left. + e^{\frac{l_1^{(n)} \rho_c^{(n)} \Omega_{g_{ci}}^{(n)} + l_2^{(n)} \Omega_{h_{ii}}^{(n)} + \phi_{i,n} (N_0 + P_{DU, I_{\text{Th}}}) \Omega_{h_{ji}}}{\phi_{i,n} \rho_c^{(n)} \Omega_{g_{ci}}^{(n)} \Omega_{h_{ji}}^{(n)}}} \Omega_{h_{ji}} \phi_{i,n} q_{i,4}^{(n)} \right), \quad (43)
 \end{aligned}$$

where

$$q_{i,1}^{(n)} = \text{Ei} \left( -\frac{l_1^{(n)}}{\mu_n \Omega_{f_{ik^*}}^{(n)}} - \frac{l_1^{(n)} (N_0 + P_{DU, I_{\text{Th}}})}{l_2^{(n)} \Omega_{h_{ii}}^{(n)}} \right) \quad (44)$$

$$q_{i,2}^{(n)} = \text{Ei} \left( \frac{(N_0 + P_{DU, I_{\text{Th}}}) (l_1^{(n)} \rho_c^{(n)} \Omega_{g_{ci}}^{(n)} + l_2^{(n)} \Omega_{h_{ii}}^{(n)})}{l_2^{(n)} \rho_c^{(n)} \Omega_{g_{ci}}^{(n)} \Omega_{h_{ii}}^{(n)}} \right), \quad (45)$$

$$q_{i,3}^{(n)} = \text{Ei} \left( -\frac{(\mu_n (N_0 + P_{DU, I_{\text{Th}}}) \Omega_{f_{ik^*}}^{(n)} + l_2^{(n)} \Omega_{h_{ii}}^{(n)})}{\mu_n l_2^{(n)} \rho_c^{(n)} \Omega_{f_{ik^*}}^{(n)} \Omega_{g_{ci}}^{(n)} \Omega_{h_{ii}}^{(n)}} \right)$$

$$\begin{aligned}
\bar{\mathbf{P}}(i) = & \sum_{n=1}^N \frac{\chi_i^n}{\Omega_{h_{ii}}^{(n)} (\mu_n \Omega_{f_{ik^*}}^{(n)} - \phi_{i,n} \Omega_{h_{ji}}^{(n)})} \left( -e^{\frac{l_1^{(n)}}{\mu_n \Omega_{f_{ik^*}}^{(n)}}} (\mu_n \Omega_{f_{ik^*}}^{(n)} (N_0 + P_{DU, I_{Th}} + \rho_c^{(n)} \Omega_{g_{ci}}^{(n)}) - l_2^{(n)} \Omega_{h_{ii}}^{(n)}) q_{i,1}^{(n)} + (N_0 + P_{DU, I_{Th}} \right. \\
& + \rho_c^{(n)} \Omega_{g_{ci}}^{(n)}) (\mu_n \Omega_{f_{ik^*}}^{(n)} - \phi_{i,n} \Omega_{h_{ji}}^{(n)}) \text{Ei} \left( -\frac{l_1^{(n)} (N_0 + P_{DU, I_{Th}})}{l_2^{(n)} \Omega_{h_{ii}}^{(n)}} \right) - e^{\frac{N_0 + P_{DU, I_{Th}}}{\rho_c^{(n)} \Omega_{g_{ci}}^{(n)}}} \mu_n \rho_c^{(n)} \Omega_{f_{ik^*}}^{(n)} \Omega_{g_{ci}}^{(n)} q_{i,2}^{(n)} + e^{\frac{N_0 + P_{DU, I_{Th}}}{\rho_c^{(n)} \Omega_{g_{ci}}^{(n)}}} \\
& \times \phi_{i,n} \rho_c^{(n)} \Omega_{g_{ci}}^{(n)} \Omega_{h_{ji}}^{(n)} q_{i,2}^{(n)} + e^{\frac{\mu_n (N_0 + P_{DU, I_{Th}}) \Omega_{f_{ik^*}}^{(n)} + l_1^{(n)} \rho_c^{(n)} \Omega_{g_{ci}}^{(n)} + l_2^{(n)} \Omega_{h_{ii}}^{(n)}}{\mu_n \rho_c^{(n)} \Omega_{f_{ik^*}}^{(n)} \Omega_{g_{ci}}^{(n)}}} \mu_n \rho_c^{(n)} \Omega_{f_{ik^*}}^{(n)} \Omega_{g_{ci}}^{(n)} q_{i,3}^{(n)} - 2l_2^{(n)} \Omega_{h_{ii}}^{(n)} q_{i,3}^{(n)} \\
& \times e^{\frac{\mu_n (N_0 + P_{DU, I_{Th}}) \Omega_{f_{ik^*}}^{(n)} + l_1^{(n)} \rho_c^{(n)} \Omega_{g_{ci}}^{(n)} + l_2^{(n)} \Omega_{h_{ii}}^{(n)}}{\mu_n \rho_c^{(n)} \Omega_{f_{ik^*}}^{(n)} \Omega_{g_{ci}}^{(n)}}} - l_2^{(n)} e^{\frac{l_1^{(n)}}{\phi_{i,n} \Omega_{h_{ji}}^{(n)}}} \Omega_{h_{ii}}^{(n)} q_{i,5}^{(n)} + e^{\frac{l_1^{(n)}}{\phi_{i,n} \Omega_{h_{ji}}^{(n)}}} \phi_{i,n} N_0 \Omega_{h_{ji}}^{(n)} q_{i,5}^{(n)} + e^{\frac{l_1^{(n)}}{\phi_{i,n} \Omega_{h_{ji}}^{(n)}}} \phi_{i,n} P_{DU, I_{Th}} \Omega_{h_{ji}}^{(n)} \\
& \times q_{i,5}^{(n)} + e^{\frac{l_1^{(n)}}{\phi_{i,n} \Omega_{h_{ji}}^{(n)}}} \phi_{i,n} \rho_c^{(n)} \Omega_{g_{ci}}^{(n)} q_{i,5}^{(n)} - e^{\frac{l_1^{(n)} \rho_c^{(n)} \Omega_{g_{ci}}^{(n)} + l_2^{(n)} \Omega_{h_{ii}}^{(n)} + \phi_{i,n} (N_0 + P_{DU, I_{Th}}) \Omega_{h_{ji}}^{(n)}}{\mu_n \rho_c^{(n)} \Omega_{f_{ik^*}}^{(n)} \Omega_{g_{ci}}^{(n)}}} (-2l_2^{(n)} \Omega_{h_{ii}}^{(n)} + \phi_{i,n} \rho_c^{(n)} \Omega_{g_{ci}}^{(n)} \Omega_{h_{ji}}^{(n)}) q_{i,4}^{(n)} \Big) \quad (49)
\end{aligned}$$

$$\begin{aligned}
& \times (l_1^{(n)} \rho_c^{(n)} \Omega_{g_{ci}}^{(n)} + l_2^{(n)} \Omega_{h_{ii}}^{(n)}) \Big) \quad (46) = \sum_{i=1}^M [f_i(\mathbf{P}^{(t-1)}) - q_i(\mathbf{P}^{(t-1)})] \quad (50)
\end{aligned}$$

$$\begin{aligned}
q_{i,4}^{(n)} = & \text{Ei} \left( -\frac{(l_1^{(n)} \rho_c^{(n)} \Omega_{g_{ci}}^{(n)} + l_2^{(n)} \Omega_{h_{ii}}^{(n)})}{l_2^{(n)} \phi_{i,n} \rho_c^{(n)} \Omega_{g_{ci}}^{(n)} \Omega_{h_{ji}}^{(n)} \Omega_{h_{ii}}^{(n)}} \right. \\
& \left. \times (l_1^{(n)} \Omega_{h_{ii}}^{(n)} + \phi_{i,n} \Omega_{h_{ji}}^{(n)} (N_0 + P_{DU, I_{Th}})) \right), \quad (47)
\end{aligned}$$

$$q_{i,5}^{(n)} = \text{Ei} \left( -\frac{l_1^{(n)}}{\phi_{i,n} \Omega_{h_{ji}}^{(n)}} - \frac{l_1^{(n)} (N_0 + P_{DU, I_{Th}})}{l_2^{(n)} \Omega_{h_{ii}}^{(n)}} \right), \quad (48)$$

in which  $l_1^{(n)} = (\nu_i + v - \eta v)$ ,  $l_2^{(n)} = (\eta \lambda + \omega_i)$  and  $\text{Ei}(x) = \int_{-\infty}^x \frac{e^t}{t} dt$  is the exponential integral function. Similarly, (21) changes to the result in equation (49), shown at the top of this page. Note that when  $J = 0$ , the channel reduces to a Rayleigh fading channel.

## B. PROOF OF THEOREM 1

*Proof:* We first prove that the expression  $\sum_{i=1}^M [f_i(\mathbf{P}^{(t)}) - q_i(\mathbf{P}^{(t)})]$  is either unchanged or improved after iteration  $t$  when the algorithm converges:

$$\begin{aligned}
& \sum_{i=1}^M [f_i(\mathbf{P}^{(t)}) - q_i(\mathbf{P}^{(t)})] \\
& \geq \sum_{i=1}^M [f_i(\mathbf{P}^{(t)}) - q_i(\mathbf{P}^{(t-1)}) - \langle \nabla q_i(\mathbf{P}^{(t-1)}), (\mathbf{P}^{(t)} - \mathbf{P}^{(t-1)}) \rangle] \\
& = \max_{\mathbf{P}} \sum_{i=1}^M [f_i(\mathbf{P}) - q_i(\mathbf{P}^{(t-1)}) - \langle \nabla q_i(\mathbf{P}^{(t-1)}), (\mathbf{P} - \mathbf{P}^{(t-1)}) \rangle] \\
& \geq \sum_{i=1}^M [f_i(\mathbf{P}^{(t-1)}) - q_i(\mathbf{P}^{(t-1)}) - \langle \nabla q_i(\mathbf{P}^{(t-1)}), (\mathbf{P}^{(t-1)} - \mathbf{P}^{(t-1)}) \rangle]
\end{aligned}$$

The first inequality follows from the fact that  $q_i(\mathbf{P})$  is a concave function, implying its gradient is also its super gradient, i.e.,

$$q_i(\mathbf{P}) \leq q_i(\mathbf{P}^{(t-1)}) + \langle \nabla q_i(\mathbf{P}^{(t-1)}), (\mathbf{P} - \mathbf{P}^{(t-1)}) \rangle$$

and we can deduce

$$q_i(\mathbf{P}^t) \leq q_i(\mathbf{P}^{(t-1)}) + \langle \nabla q_i(\mathbf{P}^{(t-1)}), (\mathbf{P}^t - \mathbf{P}^{(t-1)}) \rangle.$$

The second inequality follows from the fact that  $\mathbf{P}^{(t-1)}$  at iteration  $(t-1)$  is the optimal solution of the convex optimization problem. The iterative process will terminate as soon as the difference between  $\mathbf{P}^{(t)}$  and  $\mathbf{P}^{(t-1)}$  becomes smaller than a predefined threshold  $\epsilon > 0$ , i.e., for all elements  $|(P_i^{(n)})^{(t)} - (P_i^{(n)})^{(t-1)}| \leq \epsilon$ ,  $i = 1, \dots, M$ ,  $n = 1, \dots, N$ . So, the DC approach converges to a locally optimal solution  $\mathbf{P}^*$  of (6), and a local maximum is obtained [57], [58]. Since the lower bound in (41) is tight when evaluated in  $\mathbf{P}^{(t-1)}$ , it can be concluded that (41) is equal to (39) for  $\mathbf{P} = \mathbf{P}^{(t-1)}$ . As a result, (41) is a monotonic increasing function, which can be solved globally using Dinkelbach's algorithm.

## REFERENCES

- [1] V. W. Wong, R. Schober, D. W. K. Ng, and L. C. Wang, *Key Technologies for 5G Wireless Systems*. Cambridge, MA, USA: Cambridge Univ. Press, 2017.
- [2] D. Feng, L. Lu, Y. Yuan-Wu, G. Y. Li, S. Li, and G. Feng, "Device-to-device communications in cellular networks," *IEEE Commun. Mag.*, vol. 52, no. 4, pp. 49–55, Apr. 2014.
- [3] J. Liu, Y. Kawamoto, H. Nishiyama, N. Kato, and N. Kadowaki, "Device-to-device communications achieve efficient load balancing in LTE-advanced networks," *IEEE Wireless Commun.*, vol. 21, no. 2, pp. 57–65, Apr. 2014.
- [4] J. Liu, S. Zhang, N. Kato, H. Ujikawa, and K. Suzuki, "Device-to-device communications for enhancing quality of experience in software defined multi-tier LTE-A networks," *IEEE Network*, vol. 29, no. 4, pp. 46–52, Jul./Aug. 2015.

- [5] X. Lin, J. G. Andrews, and A. Ghosh, "Spectrum sharing for device-to-device communication in cellular networks," *IEEE Trans. Wireless Commun.*, vol. 13, no. 12, pp. 6727–6740, Dec. 2014.
- [6] W. Sun, J. Liu, Y. Yue, and Y. Jiang, "Social-aware incentive mechanisms for D2D resource sharing in IoT," *IEEE Trans. Ind. Inform.*, vol. 16, no. 8, pp. 5517–5526, Aug. 2020.
- [7] W. Sun, J. Liu, and Y. Yue, "AI-enhanced offloading in edge computing: When machine learning meets industrial IoT," *IEEE Network*, vol. 33, no. 5, pp. 68–74, Sep. 2019.
- [8] X. Liu *et al.*, "Transceiver design and multihop D2D for UAV IoT coverage in disasters," *IEEE Internet Things J.*, vol. 6, no. 2, pp. 1803–1815, Apr. 2019.
- [9] W. Sun, J. Liu, Y. Yue, and H. Zhang, "Double auction-based resource allocation for mobile edge computing in industrial Internet of Things," *IEEE Trans. Ind. Inform.*, vol. 14, no. 10, pp. 4692–4701, Oct. 2018.
- [10] J. Xie, Y. Jia, Z. Chen, Z. Nan, and L. Liang, "D2D computation offloading optimization for precedence-constrained tasks in information-centric IoT," *IEEE Access*, vol. 7, pp. 94888–94898, 2019.
- [11] Q. Wu, G. Y. Li, W. Chen, D. W. K. Ng, and R. Schober, "An overview of sustainable green 5G networks," *IEEE Wireless Commun.*, vol. 24, no. 4, pp. 72–80, Aug. 2017.
- [12] J. Zhang, E. Björnson, M. Matthaiou, D. W. K. Ng, H. Yang, and D. J. Love, "Prospective multiple antenna technologies for beyond 5G," *IEEE J. Sel. Areas Commun.*, pp. 1–20, Jun. 2020.
- [13] X. Chen, D. W. K. Ng, W. Yu, E. G. Larsson, N. Al-Dhahir, and R. Schober, "Massive access for 5G and beyond," Feb. 2020. [Online]. Available: <http://arxiv.org/abs/2002.03491>
- [14] C. Han *et al.*, "Green radio: Radio techniques to enable energy efficient wireless networks," *IEEE Commun. Mag.*, vol. 49, no. 6, pp. 46–54, Jun. 2011.
- [15] R. Mahapatra, Y. Nijssure, G. Kaddoum, N. Ul Hassan, and C. Yuen, "Energy efficiency tradeoff mechanism towards wireless green communication: A survey," *IEEE Commun. Surveys Tuts.*, vol. 18, no. 1, pp. 686–705, Jan.–Mar. 2016.
- [16] J. Wen, C. Ren, and A. K. Sangaiah, "Energy-efficient device-to-device edge computing network: An approach offloading both traffic and computation," *IEEE Commun. Mag.*, vol. 56, no. 9, pp. 96–102, Sep. 2018.
- [17] L. Xu, C. Jiang, Y. Shen, T. Q. S. Quek, Z. Han, and Y. Ren, "Energy efficient D2D communications: A perspective of mechanism design," *IEEE Trans. Wireless Commun.*, vol. 15, no. 11, pp. 7272–7285, Nov. 2016.
- [18] Q. Wu, G. Y. Li, W. Chen, and D. W. K. Ng, "Energy-efficient D2D overlaying communications with spectrum-power trading," *IEEE Trans. Wireless Commun.*, vol. 16, no. 7, pp. 4404–4419, Jul. 2017.
- [19] R. Zhang, Y. Li, C. Wang, Y. Ruan, and H. Zhang, "Performance tradeoff in relay aided D2D-cellular networks," *IEEE Trans. Veh. Technol.*, vol. 67, no. 10, pp. 10144–10149, Oct. 2018.
- [20] R. Zhang, Y. Li, C. Wang, Y. Ruan, Y. Fu, and H. Zhang, "Energy-spectral efficiency tradeoff in underlaying mobile D2D communications: An economic efficiency perspective," *IEEE Trans. Wireless Commun.*, vol. 17, no. 7, pp. 4288–4301, Jul. 2018.
- [21] A. Sultana, L. Zhao, and X. Fernando, "Efficient resource allocation in device-to-device communication using cognitive radio technology," *IEEE Trans. Veh. Technol.*, vol. 66, no. 11, pp. 10024–10034, Nov. 2017.
- [22] Y. Hao, Q. Ni, H. Li, S. Hou, and G. Min, "Interference-aware resource optimization for device-to-device communications in 5G networks," *IEEE Access*, vol. 6, pp. 78437–78452, 2018.
- [23] J. Dai, J. Liu, Y. Shi, S. Zhang, and J. Ma, "Analytical modeling of resource allocation in D2D overlaying multihop multichannel uplink cellular networks," *IEEE Trans. Veh. Technol.*, vol. 66, no. 8, pp. 6633–6644, Aug. 2017.
- [24] J. Liu, S. Zhang, H. Nishiyama, N. Kato, and J. Guo, "A stochastic geometry analysis of D2D overlaying multi-channel downlink cellular networks," in *Proc. IEEE INFOCOM*, May 2015, pp. 46–54.
- [25] M. Peng, Y. Li, T. Q. S. Quek, and C. Wang, "Device-to-device underlaid cellular networks under Rician fading channels," *IEEE Trans. Wireless Commun.*, vol. 13, no. 8, pp. 4247–4259, Aug. 2014.
- [26] Y. Wang, M. Chen, N. Huang, Z. Yang, and Y. Pan, "Joint power and channel allocation for D2D underlaying cellular networks with Rician fading," *IEEE Commun. Lett.*, vol. 22, no. 12, pp. 2615–2618, Dec. 2018.
- [27] K. Miettinen, *Nonlinear Multiobjective Optimization*. Norwell, MA, USA: Kluwer, 1998.
- [28] M. R. Mili, A. Khalili, D. W. K. Ng, and H. Steendam, "A novel performance tradeoff in heterogeneous networks: A multi-objective approach," *IEEE Wireless Commun. Lett.* vol. 8, no. 5, pp. 1402–1405, Oct. 2019.
- [29] C. Vlachos and V. Friderikos, "MOCA: Multiobjective cell association for device-to-device communications," *IEEE Trans. Veh. Technol.*, vol. 66, no. 10, pp. 9313–9327, Oct. 2017.
- [30] M. R. Mili, F. Mokhtari, and F. Ashtiani, "Improving tradeoff among downlink rates of service providers in a VWN by using NOMA," *IEEE Commun. Lett.*, vol. 23, no. 1, pp. 156–159, Jan. 2019.
- [31] A. Khalili, M. R. Mili, M. Rasti, S. Parsaeefard, and D. W. K. Ng, "Antenna selection strategy for energy efficiency maximization in uplink OFDMA networks: A multi-objective approach," *IEEE Trans. Wireless Commun.* vol. 19, no. 1, pp. 595–609, Jan. 2020.
- [32] A. Khalili, M. R. Mili, and D. W. K. Ng, "Performance trade-off between uplink and downlink in full-duplex communications," Feb. 2020. [Online]. Available: <http://arxiv.org/abs/2002.07406>
- [33] M. R. Mili and L. Musavian, "Interference efficiency: A new performance metric for cognitive radio networks," *IEEE Trans. Wireless Commun.*, vol. 16, no. 4, pp. 2123–2138, Apr. 2017.
- [34] J. Rubio, A. Pascual-Iserte, D. P. Palomar, and A. Goldsmith, "Joint optimization of power and data transfer in multiuser MIMO Systems," *IEEE Trans. Signal Process.*, vol. 65, no. 1, pp. 212–227, Jan. 2017.
- [35] M. R. Mili, L. Musavian, K. A. Hamdi, and F. Marvasti, "How to increase energy efficiency in cognitive radio networks," *IEEE Trans. Commun.*, vol. 64, no. 5, pp. 1829–1843, May 2016.
- [36] A. Khalili and D. W. K. Ng, "Energy and spectral efficiency tradeoff in OFDMA networks via antenna selection strategy," in *Proc. IEEE Wireless Commun. Netw. Conf.*, Seoul, Korea (South), Feb. 2020, pp. 1–6.
- [37] O. Aydin, E. A. Jorswieck, D. Aziz, and A. Zappone, "Energy-spectral efficiency tradeoffs in 5G multi-operator networks with heterogeneous constraints," *IEEE Trans. Wireless Commun.*, vol. 16, no. 9, pp. 5869–5881, Sep. 2017.
- [38] Y. Hao, Q. Ni, H. Li, and S. Hou, "Robust multi-objective optimization for EE-SE tradeoff in D2D communications underlying heterogeneous networks," *IEEE Trans. Commun.*, vol. 66, no. 10, pp. 4936–4949, Oct. 2018.
- [39] N. Mokari, P. Azmi, and H. Saeedi, "Quantized ergodic radio resource allocation in cognitive networks with guaranteed quality of service for primary network," *IEEE Trans. Veh. Technol.*, vol. 63, no. 8, pp. 3774–3782, Oct. 2014.
- [40] D. W. K. Ng, E. S. Lo, and R. Schober, "Energy-efficient resource allocation in multi-cell OFDMA systems with limited backhaul capacity," *IEEE Trans. Wireless Commun.*, vol. 11, no. 10, pp. 3618–3631, Oct. 2012.
- [41] Wei Yu and R. Lui, "Dual methods for nonconvex spectrum optimization of multicarrier systems," *IEEE Trans. Commun.*, vol. 54, no. 7, pp. 1310–1322, Jul. 2006.
- [42] S. Boyd and L. Vandenberghe, *Convex Optimization*. Cambridge, UK: Cambridge Univ. Press, 2004.
- [43] M. Tao, Y.-C. Liang, and F. Zhang, "Resource allocation for delay differentiated traffic in multiuser OFDM systems," *IEEE Trans. Wireless Commun.*, vol. 7, no. 6, pp. 2190–2201, Jun. 2008.
- [44] D. P. Bertsekas, *Nonlinear Programming*, 2nd ed. Belmont, MA, USA: Athena Scientific, 1999.
- [45] D. P. Bertsekas, A. Nedic, and A. E. Ozdaglar, *Convex Analysis and Optimization*. Belmont, MA, USA: Athena Scientific, 2003.
- [46] I. S. Gradshteyn and I. M. Ryzhik, *Table of Integrals, Series, and Products*, 7th ed. San Diego, CA, USA: Academic, 2007.
- [47] Z. Q. Luo and S. Zhang, "Dynamic spectrum management: Complexity and duality," *IEEE J. Sel. Top. signal Process.*, vol. 2, no. 1, pp. 57–72, Feb. 2008.
- [48] H. H. Kha, H. D. Tuan, and H. H. Nguyen, "Fast global optimal power allocation in wireless networks by local DC programming," *IEEE Trans. Wireless Commun.*, vol. 11, no. 2, pp. 510–515, Feb. 2012.
- [49] M. Frank and P. Wolfe, "An algorithm for quadratic programming," *Naval Res. Logist. Quart.*, vol. 3, pp. 95–110, 1956.
- [50] N. N. Lebedev and R. Silverman, *Special Functions and Their Applications*. New York, NY, USA: Dover, 1972.
- [51] A. Ghasemi and E. S. Sousa, "Fundamental limits of spectrum-sharing in fading environments," *IEEE Trans. Wireless Commun.*, vol. 6, no. 2, pp. 649–658, Feb. 2007.
- [52] W. Dinkelbach, *On Nonlinear Fractional Programming*, Management Science, vol. 13, no. 7, pp. 492–498, 1967.
- [53] A. Zappone, E. Björnson, L. Sanguinetti, and E. Jorswieck, "Globally optimal energy-efficient power control and receiver design in wireless networks," *IEEE Trans. Signal Process.*, vol. 65, no. 11, pp. 2844–2859, Jun. 2017.
- [54] A. Khalili, S. Zrandi, and M. Rasti, "Joint resource allocation and offloading decision in mobile edge computing," *IEEE Commun. Lett.*, vol. 23, no. 4, pp. 684–687, Apr. 2019.

- [55] R. Aslani, M. Rasti, and A. Khalili, "Energy efficiency maximization via joint sub-carrier assignment and power control for OFDMA full duplex networks," *IEEE Trans. Veh. Technol.*, vol. 68, no. 12, pp. 11859–11872, Dec. 2019.
- [56] A. L. Yuille and A. Rangarajan, "The concave-convex procedure," *Neural Computation*, vol. 15, no. 4, pp. 915–936, Apr. 2003.
- [57] A. Khalili, S. Akhlaghi, H. Tabassum, and D. W. K. Ng, "Joint user association and resource allocation in the uplink of heterogeneous networks," *IEEE Wireless Commun. Lett.*, vol. 9, no. 6, pp. 804–808, Jun. 2020.
- [58] A. Khalili, S. Zarandi, M. Rasti, and E. Hossain, "Multi-objective optimization for energy- and spectral-efficiency tradeoff in in-band full-duplex (IBFD) communication," in *Proc. IEEE Globecom* Dec. 2019, pp. 1–6.



**Mohammad Robot Mili** received the Ph.D. degree in electrical and electronic engineering from the University of Manchester, U.K., in 2012. He held postdoctoral research positions at the Department of Telecommunications and Information Processing, Ghent University, Belgium and the Department of Electrical Engineering, Sharif University of Technology, Iran. His main research interests are in the area of design and analysis of wireless communication networks with particular focus on 5G cellular networks using mathematical methods such as optimization theory, game theory, and machine learning.



**Ata Khalili** (Graduate Student Member, IEEE) received the B.Sc. and M.Sc. degrees with first class honors in electronic engineering and telecommunication engineering from Shahed University, in 2016 and 2018, respectively. From 2018 until 2019, he was a Visiting Researcher at the Department of Computer Engineering and Information Technology, Amirkabir University of Technology, Tehran, Iran. Since October 2019, he has been at the Department of Electrical and Computer Engineering, Tarbiat Modares University, Tehran, Iran, where he is currently a Research

Assistant. He is also working as a Research Assistant at the Electronics Research Institute, Sharif University of Technology, Tehran, Iran. His research interests include intelligent reflecting surface (IRS), unmanned aerial vehicle (UAV) communications, resource allocation in wireless communication, green communication, mobile edge computing, and optimization theory. He served as a member of Technical Program Committees for the IEEE Globecom Conference in 2020.



**Nader Mokari** (Senior Member, IEEE) received the Ph.D. degree in electrical engineering from Tarbiat Modares University, Tehran, Iran, in 2014. He joined the Department of Electrical and Computer Engineering, Tarbiat Modares University, as an Assistant Professor, in 2015. Now, he is an Associated Professor at the Department of Electrical and Computer Engineering, Tarbiat Modares University, Tehran, Iran. He was involved in a number of large-scale network design and consulting projects in the telecom industry. His research interests include design, analysis, and

optimization of communication networks, and machine learning.



**Sabine Wittevrongel** received the master's degree in electrical engineering and the Ph.D. degree in engineering from Ghent University, Belgium, in 1992 and 1998 respectively. In 1992, she joined the SMACS Research Group of the Department of Telecommunications and Information Processing at Ghent University. In 1998, she received the Scientific Award Alcatel Bell for the work entitled "Generic analytical techniques for the performance analysis of buffers in ATM networks." Since 2001, she is a Professor in the field of stochastic modeling and queueing analysis

in the Faculty of Engineering and Architecture at Ghent University. Her main research interests include queueing theory, stochastic modeling and performance evaluation of communication networks, scheduling mechanisms and energy-efficient protocols.



**Derrick Wing Kwan Ng** (Senior Member, IEEE) received the bachelor's degree with first-class honors and the M.Phil. degree in electronic engineering from the Hong Kong University of Science and Technology (HKUST), in 2006 and 2008, respectively, and the Ph.D. degree from the University of British Columbia (UBC), in 2012. He was a Senior Postdoctoral Fellow at the Institute for Digital Communications, Friedrich-Alexander-University Erlangen-Nürnberg (FAU), Germany. He is now working as a Senior Lecturer and an ARC DECRA Research

Fellow at the University of New South Wales, Sydney, Australia. His research interests include convex and non-convex optimization, physical layer security, wireless information and power transfer, and green (energy-efficient) wireless communications. Dr. Ng received the Best Paper Awards at the IEEE TCGCC Best Journal Paper Award 2018, INISCOM 2018, IEEE International Conference on Communications (ICC) 2018, IEEE International Conference on Computing, Networking and Communications (ICNC) 2016, IEEE Wireless Communications and Networking Conference (WCNC) 2012, the IEEE Global Telecommunication Conference (Globecom) 2011, and the IEEE Third International Conference on Communications and Networking in China 2008. He has been serving as an Editorial Assistant to the Editor-in-Chief of the IEEE TRANSACTIONS ON COMMUNICATIONS since January 2012. In addition, he is listed as a Highly Cited Researcher by Clarivate Analytics in 2018 and 2019.



**Heidi Steendam** (Senior Member, IEEE) received the M.Sc. degree in electrical engineering and the Ph.D. degree in applied sciences from Ghent University, Ghent, Belgium, in 1995 and 2000, respectively. Since 1995, she has been with the Digital Communications Research Group, Department of Telecommunications and Information Processing, Faculty of Engineering, Ghent University, in the framework of various research projects, and has been a Professor in digital communications since 2002. In 2015, she was a Visiting Professor with Monash University.

She has authored more than 150 scientific papers in international journals and conference proceedings, for which she received several best paper awards. Her main research interests are in statistical communication theory, carrier and symbol synchronization, bandwidth-efficient modulation and coding, cognitive radio and cooperative networks, and positioning and visible light communication. Dr. Steendam has been an Executive Committee Member of the IEEE Communications and Vehicular Technology Society Joint Chapter, Benelux Section, since 2002, the Vice Chair since 2012, and the Chair since 2017. She was active in various international conferences as a Technical Program Committee Chair/Member and the Session Chair. In 2004 and 2011, she was the Conference Chair of the IEEE Symposium on Communications and Vehicular Technology in the Benelux. From 2012 to 2017, she was an Associate Editor of the IEEE TRANSACTIONS ON COMMUNICATIONS and the *EURASIP Journal on Wireless Communications and Networking*.